NOTE TO USERS

Liquefaction Potential Assessment in Soil Deposits Using Artificial Neural Networks

Gokhan Saygili

A Thesis

in

The Department

Of

Building, Civil, and Environmental Engineering

Presented in Partial Fulfillment of the Requirements
For the Degree of Master of Applied Science at
Concordia University
Montreal, Quebec, Canada

May 2005

Your file Votre référence
ISBN: 0-494-04357-1
Our file Notre référence
ISBN: 0-494-04357-1

ABSTRACT

Liquefaction Potential Assessment in Soil Deposits Using Artificial Neural Networks

Gokhan Saygili

In the literature, several simplified methods can be found to assess nonlinear liquefaction potential of soil. Derived from several field and laboratory tests, various procedures, also named as conventional methods, have been developed by utilizing case studies and undisturbed soil samples. In order to examine the collective knowledge built up in the conventional liquefaction methods available in the literature, a General Regression Neural Network (GRNN) model is proposed herein, which incorporates the parameters ignored in the past and accordingly will eliminate the shortcomings of the existing design formulae.

Two separate sets of field data, based on the standard penetration test, SPT, and the cone penetration test, CPT were used to develop the GRNN model. A total of 620 case records for SPT data, and 3895 case records for CPT data were collected and utilized to develop the GRNN. This data includes the results of field tests collected from the two major earthquakes that took place in Turkey and Taiwan in 1999. These case records were divided randomly into testing, training, and validation datasets. The GRNN was then tested by twenty-four soil and seismic parameters; twelve of which are used in the SPT database and twelve of which are used in the CPT database, where good performance was observed. Additional input parameters are obtained from correlations existing in the literature. Soil liquefaction decisions in terms of seismic demand and seismic capacity are determined by recognized simplified approach, namely stress-

based method and strain-based method. Furthermore, liquefaction probability of soils with significant fines was tested with the so-called Chinese Criteria. An iterative procedure was followed to maximize the accuracy of the proposed models.

The proposed GRNN model predicted the occurrence/nonoccurrence of soil liquefaction well in these sites. Furthermore, liquefaction decision supported by SPT test results is incorporated into CPT based soil and seismic data. Therefore, the model supports the data conversion of an SPT-to-CPT throughout the liquefaction potential analysis, which believed to be the primary limitation of the simplified techniques. Thus the proposed model provides a viable tool to geotechnical engineers in assessing seismic condition in sites susceptible to liquefaction.

ACKNOWLEDGEMENT

I would like to acknowledge my supervisor Dr. A.M. Hanna for his tremendous effort in advising, teaching and supporting me throughout this research and giving me the chance to study under his supervision. I would also like to acknowledge Dr. Derin (Ural) Serpenguzel's continuing feedback and insights throughout the development of this research.

TABLE OF CONTENTS

LIST OF FIGURES

LIST OF TABLES

LIST OF SYMBOLS

Symbol	Description
AI	Artificial intelligence
ANN	Artificial neural network
a_{max}	Peak horizontal acceleration at ground surface
a_t	Threshold acceleration
BPNN	Back propagation neural network
C_B	Correction for Bore Hole Diameter
C_E	Correction for Hammer Energy Ratio
C_N	Correction for Effective Overburden Stress
C_R	Correction for Rod Length
C_S	Correction for Samplers
CSR	Cyclic stress ratio
$CRR_{7.5}$	Cyclic resistance ratio for the magnitude 7.5 earthquakes
d_w	Depth of ground water table
ER	Hammer energy ratio
F≤75 μm	Percent fines less than 75 μm
f_s	CPT sleeve friction resistance
GRNN	General regression neural network
H_0	Null hypothesis
IBL	Instance based learning models

LL	Liquid limit
MSF	Magnitude scaling factor
M_v	Earthquake magnitude
Max	Maximum value
Min	Minimum value
$(N_1)_{60}$	Corrected standard penetration blow number
$(N_1)_{60,cs}$	Correlated SPT-N value for Finest Content
P	Probability
PI	Plasticity index
q_c	CPT Cone tip resistance
R_f	CPT friction ratio
r_d	Stress Reduction Factor
SNN	Sequential neural network
S	Standard Deviation
V_s	Shear wave velocity
w	Moisture content
z	Depth of soil specimen
α	Significance level
ϕ'	Internal friction angle of soil
$\left(\frac{G}{G_{max}}\right)_t$	Modulus reduction factor at the threshold strain, γ_t
μ	Mean value

γ_τ	Threshold strain
σ	Smoothing factor, or bandwidth
σ_{vo}	Total vertical stress
σ'_{vo}	Effective vertical stress
$\frac{\tau_{av}}{\sigma'_{vo}}$	Cyclic stress ratio
$\hat{Y}$	GRNN output

CHAPTER I

INTRODUCTION

1.1 GENERAL

In soils under undrained condition; earthquakes induce cyclic shear stresses, which may lead to soil liquefaction. This can be explained by the fact that in a liquefiable soil layer, under dynamic loads the pore water pressure increases suddenly, leading to a significant reduction in its shear strength and accordingly to liquefaction of the soil layer. By definition, soil liquefaction is the loss of shear strength due to a transfer of intergranular stress from grains to pore water (Seed 1979).

Liquefaction has vital importance on the serviceability of bridges, railway embankments, airport runways, submerged tunnels, buried structures such as water, sewage, gas pipelines, and underground electric power and telecommunication lines. Therefore, it is important to predict the liquefaction potential and to take precautions against liquefaction in susceptible sites.

There are many examples of serious damage caused by liquefaction in earthquakes such as the sudden loss of bearing capacity of foundations, floating of buried structures, dislocation of retaining walls and the excessive lateral soil movement.

Since the effect of this phenomenon on human life and the economy is significant, geotechnical engineers have given their interest to investigate this problem. The two basic approaches that have been implemented to assess liquefaction potential in layered soil are (Seed and Idriss 1971, De Alba et. al. 1976, Seed 1979, Seed et. al. 1983):

a. **Laboratory tests**: They are based on cyclic stress and strain comparisons of soil samples. Laboratory based techniques are believed to yield less reliable results due to both disturbance of the specimens and the high costs.

b. **Empirical methods**: They are based on observations in previous earthquakes. Currently, liquefaction-engineering procedures profoundly rely on empirical correlations such as cyclic stress ratio for stress-based methodology and threshold acceleration for strain-based methodology. Accordingly, parameters derived from field tests are used directly through empirical calculations. These correlations derived from case histories yield relatively more reliable results than laboratory tests.

1.2 PROBLEM DEFINITION

Over the last 30 years, simplified methods, developed from empirical equations and laboratory tests data have become a general practice for the evaluation of soil liquefaction in layered soils. Apart from being cost efficient, simplified methods based on in-situ and/or laboratory test results provide engineers with a reliable prediction of soil liquefaction. This research focuses on the evaluation of soil liquefaction in layered soils by presenting an alternative computational tool to the ongoing empirical approach.

1.3 RESEARCH OBJECTIVE

Soil liquefaction evaluations can be successfully achieved by employing all the governing soil and seismic parameters in one single model. Therefore, in this study, a comprehensive

approach that consists of all independent soil and seismic parameters proven to be influential for decision making are taken into account. In that respect, Artificial Networks are proven to be capable to incorporate a wide variety of parameters, representing a serious alternative to the available models. The objective of this research can be summarized as follows:

1. To conduct a literature review on the existing simplified models for predicting soil liquefaction and highlight the limitations of these models by presenting conceptual mechanism of soil liquefaction.
2. To generate a massive dataset of governing parameters that affects the soil liquefaction obtained from the 1999 Chi-Chi, Taiwan earthquake (Magnitude M_v=7.6) region and the 1999 Kocaeli, Turkey earthquake (magnitude M_v=7.4) region.
3. To develop a Neural Network that incorporates all the influential factors and actual data to predict soil liquefaction potential in layered soils.

1.4 THESIS ORGANIZATION

This thesis is organized as follows:

Chapter 2: Literature Review: This chapter presents a brief discussion on the existing simplified methods proposed by different researchers for assessing soil liquefaction potential.

Chapter 3: Analyses of Data: This chapter presents the SPT and CPT data sets and presents a concise version to generate the databases.

Chapter 4: Artificial Network Model: This chapter introduces Artificial Neural Networks (ANN) as a model to predict the liquefaction potential. It also presents the GRNN model, which

was developed in four phases; these are: identification phase, collection phase, implementation phase and verification phase.

Chapter 5: Conclusions and Recommendations: This chapter highlights the contribution of this research and suggests recommendations for future work.

CHAPTER 2

LITERATURE REVIEW

2.1 GENERAL

The evaluation of the soil liquefaction potential has been a challenging task to geotechnical engineers, especially after the two disastrous earthquakes, namely the 1964 Niigata earthquake (Japan) and 1964 Great Alaskan earthquake (US). In the literature soil liquefaction potential has been classified to include the development of instrumentation and cost-efficient field observations. The current research trends have focused on four in-situ tests. These are:

1. Standard Penetration Test (SPT)
2. Cone Penetration Test (CPT)
3. Shear Wave Velocity Test
4. Becker Penetration Test (BPN)

The following chapter will present the historical development of existing SPT based empirical methods in the literature.

2. 2 HISTORICAL DEVELOPMENT OF SIMPLIFIED METHODS

Following the devastating earthquakes in US and Japan in 1964, researchers started to investigate the use of the SPT to develop empirical methods. Starting in the 1970s, Seed (1971) has initiated the empirical approach by generating the so-called "Simplified Method", which was followed by numerous researchers to shape that empirical approach.

Seed and Idriss (1971) formulated the shear stresses in any soil deposit during an earthquake, as follows;

$$(\tau_{max})_r = \frac{\gamma h}{g} a_{max} \quad (2.1)$$

Where,

$(\tau_{max})_r$ = maximum shear stress

h = height of the soil column above a soil element

γ = unit weight of the soil

g = acceleration of gravity

a_{max} = maximum horizontal ground surface acceleration

Since the soil column is not a rigid body and is subjected to deformations, the actual shear stress evaluation requires a nonlinear shear mass participation factor. The relation is given as;

$$(\tau_{max})_d = (\tau_{max})_r r_d \quad (2.2)$$

Where,

$(\tau_{max})_d$ = actual shear stress

$(\tau_{max})_r$ = maximum shear stress

r_d = the nonlinear shear mass participation factor

r_d is also called as stress reduction factor with a value less than unity. The variation of the nonlinear shear mass participation factor with respect to increasing soil depth is given in Figure 2.1.

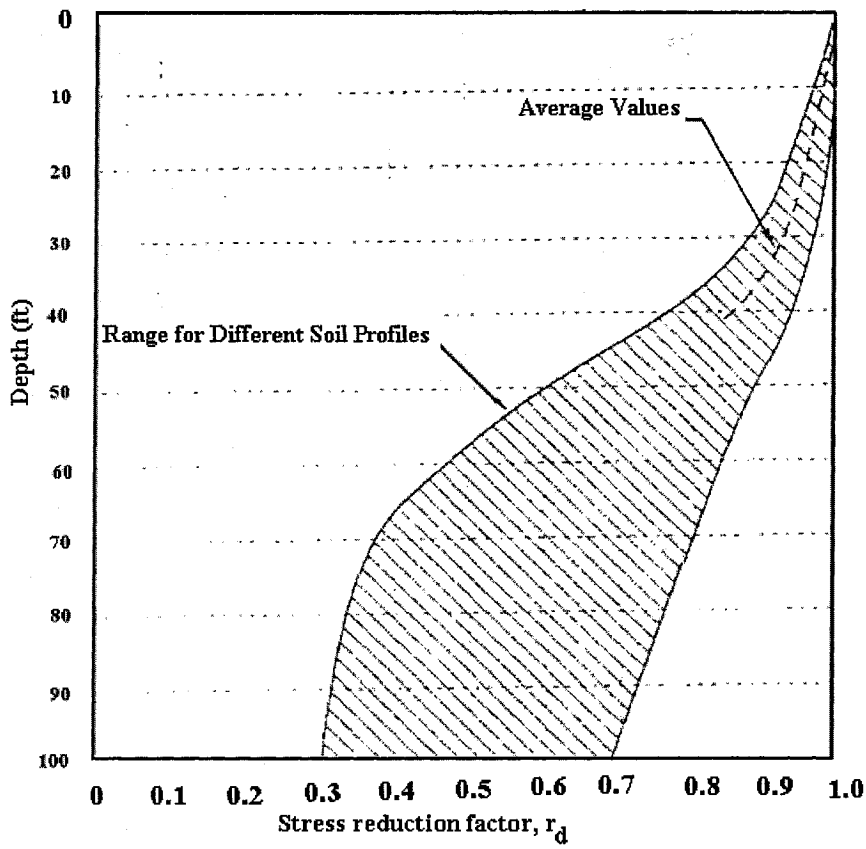

Figure 2.1: Stress reduction factor (Seed and Idriss 1971)

Seed and Idriss (1971) formulated the cyclic stress ratio (CSR) developed on a soil element in the field during an earthquake as follows:

$$CSR_{peak} = \tau_{av} / \sigma'_{vo} = \left(\frac{a_{\max}}{g}\right)\left(\frac{\sigma_{vo}}{\sigma'_{vo}}\right) r_d \qquad (2.3)$$

Where,

a_{max} = maximum horizontal ground surface acceleration

g = acceleration of gravity

r_d = the nonlinear shear mass participation factor

σ_{vo}= total vertical overburden stress

σ'_{vo}= effective vertical overburden stress

Based on laboratory test data of Seed and Idriss (1971), the average equivalent uniform shear stress is about 65 percent of the maximum shear stress. Therefore, the average cyclic shear stress may be determined as;

$$CSR_{eq.} = (0.65)CSR_{peak} \tag{2.4}$$

Where,

CSR_{eq} = Equivalent cyclic stress ratio

CSR_{peak} = Peak cyclic stress ratio

Seed and Idriss (1971) developed a standard penetration test number (SPT-N) versus cyclic stress ratio (CSR) curve.

The main limitations of the simplified method developed by Seed and Idriss (1971) are:

a. In the liquefaction boundary curve, there was a limited amount of reliable data to define the boundary separating liquefiable and non-liquefiable sites. This problem has been partly solved by ongoing research, which will be discussed later in this chapter.

b. The stress reduction coefficient has proven to provide biased (generally high) estimates of r_d at depths between 3 to 15 m. (Seed et. al. 2003; Youd et. al. 2001)

Seed et. al. (1977) proposed a correlation between the stress ratio and SPT penetration resistance by utilizing additional data from the results of Christian and Swinger (1975). Like previous studies, the main limitation of this correlation was lack of reliable data. Besides, the results were not applicable due to changing of the initial conditions of the ground water level and chancing shaking intensities. The correlation curve is given in Figure 2.2.

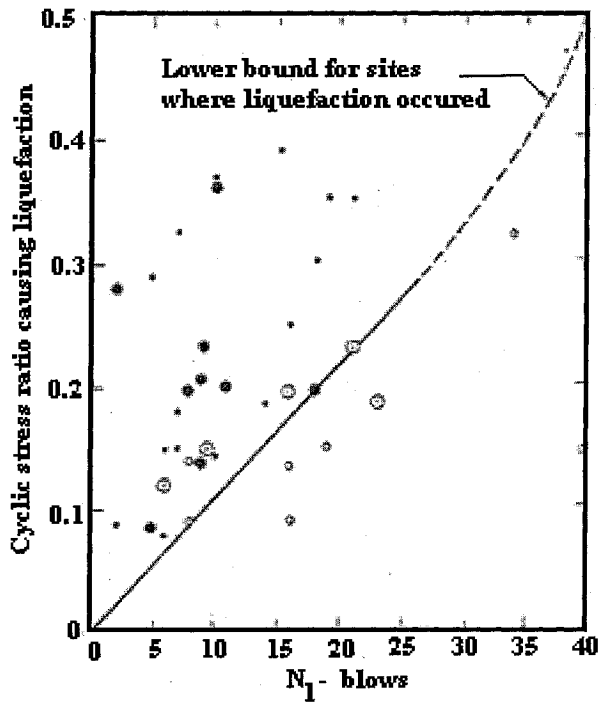

Figure 2.2: Correlation between stress ratio causing liquefaction in the field and the penetration resistance (Seed et. al. 1977)

Seed and Idriss (1982) produced a revised boundary curve by advancing the previous dataset (Seed and Idriss 1971). The boundary curve had a far greater degree of confidence (Figure 2.3).

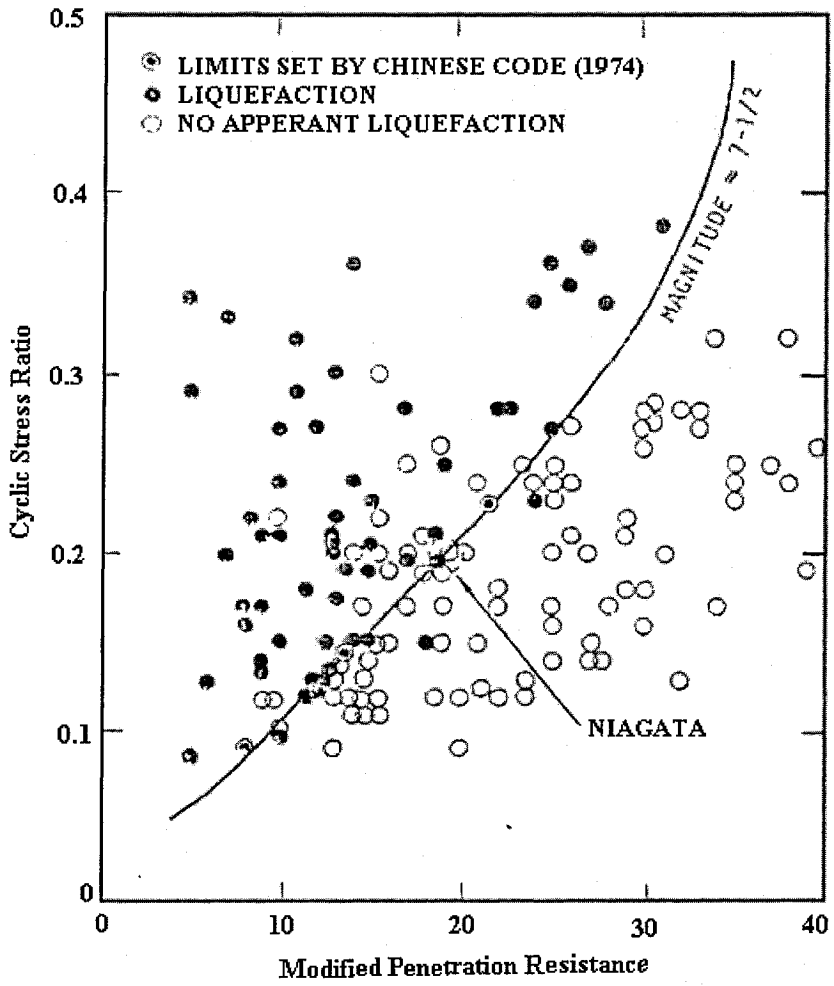

Figure 2.3: Field liquefaction of sands (D50 > 0.25mm) versus SPT resistance

(Seed et. al. 1982)

The soil data utilized to draw Figure 2.3 were taken from a series of earthquakes, which have magnitudes of 7.5. Therefore, a magnitude correction factor was introduced and given in Figure 2.4.

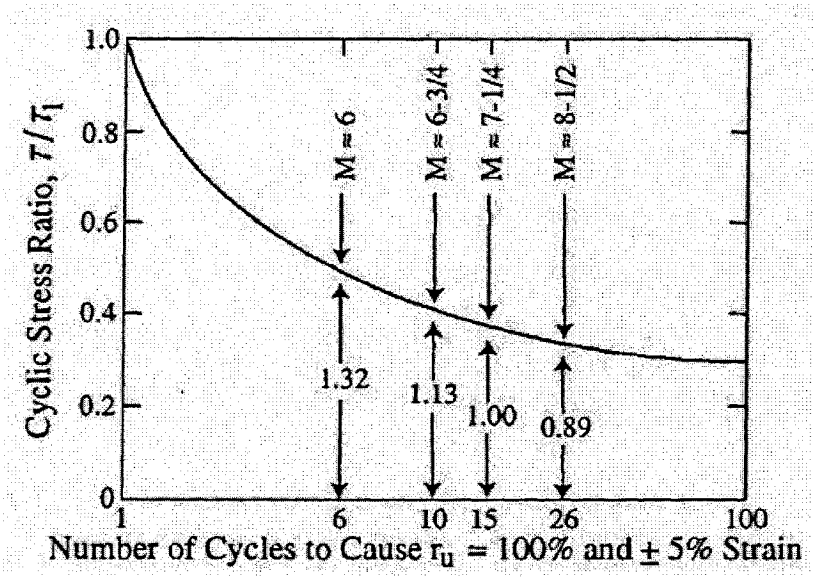

Figure 2.4: Earthquakes magnitude scaling factor and its relationship between CSR and Number of Cycles to cause Liquefaction (Seed et. al. 1982)

Seed and Idriss (1982) concluded that the standard penetration resistance increases with increasing the effective overburden stress and further they presented the "C_N" factor curve to normalize the measured standard penetration resistance.

Figure 2.5, shows the "Modified Chinese Criteria" presented by Seed and Idriss (1981, 1982), Seed et. al. (1983) and Wang (1979). In this Figure, the finest content liquefaction potential assessment criteria indicates that soils with a significant plasticity are considered vulnerable to significant loss of strength or liquefaction if they fall into one of these three categories;

a. Percent finer than 0.005 mm $\leq$ 15%

b. Liquid limit (LL) $\leq$ 35%

c. Water content (W) $\leq$ 0.9 x LL

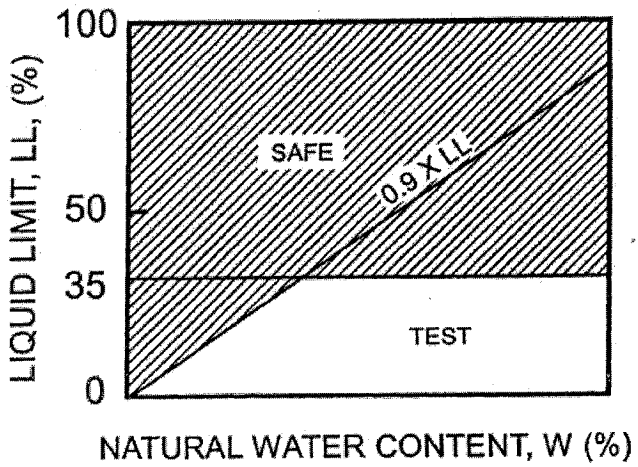

Figure 2.5: Modified Chinese criteria (Wang 1979 and Seed and Idriss 1982)

The main limitation of the Seed and Idriss (1982) procedure are;

a. The original curve (Figure 2.3) was projected to the origin, although there are few points in the lower part of the plot. (Youd et. al. 2001)

b. Due to a limited amount of earthquake data from sites different than a 7.5 magnitude, the magnitude scaling factor curve (Figure 2.4) is unable to adequately contain boundaries between liquefaction and non-liquefaction regions for magnitudes other than 7.5 (Youd et. al. 2001)

c. C_N should not exceed a value of 1.7 (Youd et. al. 2001)

d. The Chinese criteria modified by numerous researchers, but still there is no common consensus reached among researchers and more study was warranted (Seed et. al. 2003)

Seed et. al. (1985) proposed a "deterministic" approach for SPT based on simplified methods and that methodology became a common practice in earthquake engineering.

The chart presented by Seed et. al. (1985) suggests a boundary curve between the cyclic stress ratio, CSR, and the standardized SPT blow-count, $(N_1)_{60}$. In order to evaluate $(N_1)_{60}$ values, SPT-N values were required to be normalized with respect to effective overburden stress and to be corrected with respect to energies delivered with respect to different types of hammer systems. The equation for SPT-N blow-count correction was given as;

$$(N_1)_{60} = (N_1)_m \frac{ER_m}{60} \tag{2.5}$$

Where:

$(N_1)_{60}$ = Standardized SPT blow-count

$(N_1)_m$ = SPT-N value normalized for effective stress

$(ER)_m$ = Rod energy ratio for the method used in investigation

Summary of Energy ratios for SPT procedures are given in Table 1.

Table 2.1: Summary of Energy Ratios for SPT (Seed et. al. 1985)

Country	***Hammer Type***	***Hammer Release***	***Estimated Rod Energy***	***Correction Factor for 60% Rod Energy***
Japan	Donut	Free-Fall	78	1.30
Japan	Donut	Rope and Pulley with Throw Release	67	1.12
USA	Safety	Rope and Pulley	60	1.00
USA	Donut	Rope and Pulley	45	0.75
Argentina	Donut	Rope and Pulley	45	0.75
China	Donut	Free-Fall	60	1.00
China	Donut	Rope and Pulley	50	0.83

Seed et. al. (1985) proposed boundary curves separating sites where liquefaction effects were or were not observed (Figure 2.6). In this Figure, the curves were developed for granular soils with the fines content of 5% or less, 15%, and 35%. These curves provide a reasonable basis for evaluating the liquefaction resistance of sands and silty sands for magnitude of 7.5 earthquakes.

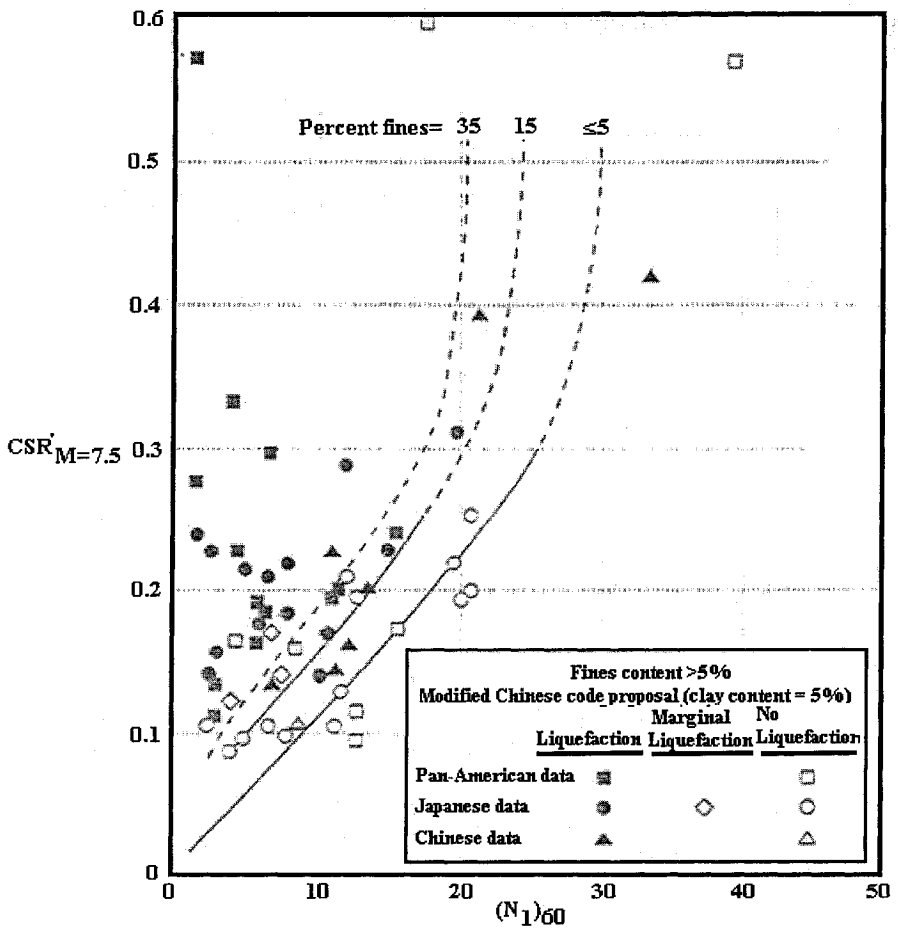

Figure 2.6: Correlation between cyclic stress ratio, CSR, and SPT $(N_1)_{60}$ value for magnitude 7.5 earthquakes (Seed et. al. 1985)

The main limitations of the Seed et. al. (1985) procedure are;

a. Instead of a single liquefaction boundary curve, transition zones were suggested; furthermore, it was proven that this approach predicted liquefaction in some cases where no liquefaction would occur (Fear and McRoberts 1995)
b. Seed et. al. (1985) indicated that CSR increases with increased fines content. However, the cause of the increase of fines whether due to the increase of liquefaction resistance or a decrease of penetration resistance, which was not clear (Youd et. al. 2001)
c. Boundary curve for fines content $\leq$ 5% corresponds to the probability of liquefaction of 50%, which is not a real case (Seed et. al. 2003)
d. The correlation of Seed et. al. (1985) was never formally corrected to σ'_v =1 atm, however, it was noted that the field case histories in the database were "shallow", and approximately in this range. (Seed et. al 2003)

Liao et. al. (1988) proposed a statistical regression analysis to correlate a liquefaction boundary curves in terms of CSR and SPT $(N_1)_{60}$ value. Figure 2.7 shows these boundary curves, which included a larger number of case history than were utilized by Seed et. al. (1985), and also probabilities of liquefaction of 5%, 20%, 50%, 80%, and 95% were given.

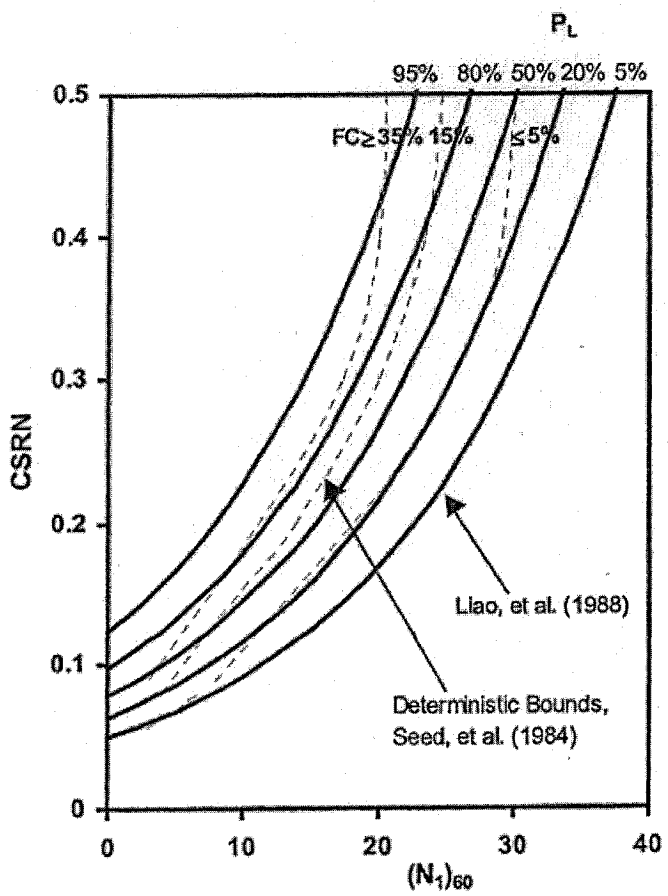

Figure 2.7: Statistical analysis for evaluation of liquefaction potential proposed by Liao et. al. (1988) (published in Seed et. al. 2003)

The main limitations of Liao et. al. (1988) procedure are

a. Although the data set utilized for liquefaction potential analysis was relatively more than the dataset used by Seed et. al. (1985), the data set included a number of low quality data. (Seed et. al 2003)

b. The proposed model failed to incorporate the impacts of fine content on the relationship between SPT blow-count and the liquefaction resistance. Therefore, only the curves for sandy soils with less than 12% fines are reliable. (Seed et. al. 2003)

Apart from the review of Seed et. al. (1985), no general update to the procedure, named as simplified method, was developed since 1985. However, Youd et. al. (2001) together with 21 experts have proposed a report of consensus recommendations including the developments that took place over the last 10 years.

Liao and Whitman (1986b) proposed the following equation for a routine and non-critical project to estimate average values of stress reduction factor;

$$r_d = 1.0 - 0.00765z \text{ for the cases of } z \leq 9.15 \text{ m} \quad (2.6a)$$

$$r_d = 1.174 - 0.0267z \text{ for the cases of } 9.15 < z \leq 23 \text{ m} \quad (2.6b)$$

Where:

z = Depth below ground surface in meters

Regarding the factor to normalize measured standard penetration resistance to a common reference effective overburden stress (C_N), Kayen et. al. (1992) proposed the following equation;

$$C_N = 2.2 / (1.2 + \sigma'_{vo}/p_a) \quad (2.7)$$

Where,

σ'_{vo} = Effective overburden stress

P_a = Atmosphere pressure (1 atm=100 kPa)

This equation limits the C_N value to 1.7 and according to the 20 experts attended to the NCEER workshop; this equation provides a suitable fit to the original curve specified by Seed

and Idriss (1982). In addition to this approximation, numerous researchers proposed C_N curves, which are given in Figure 2.8.

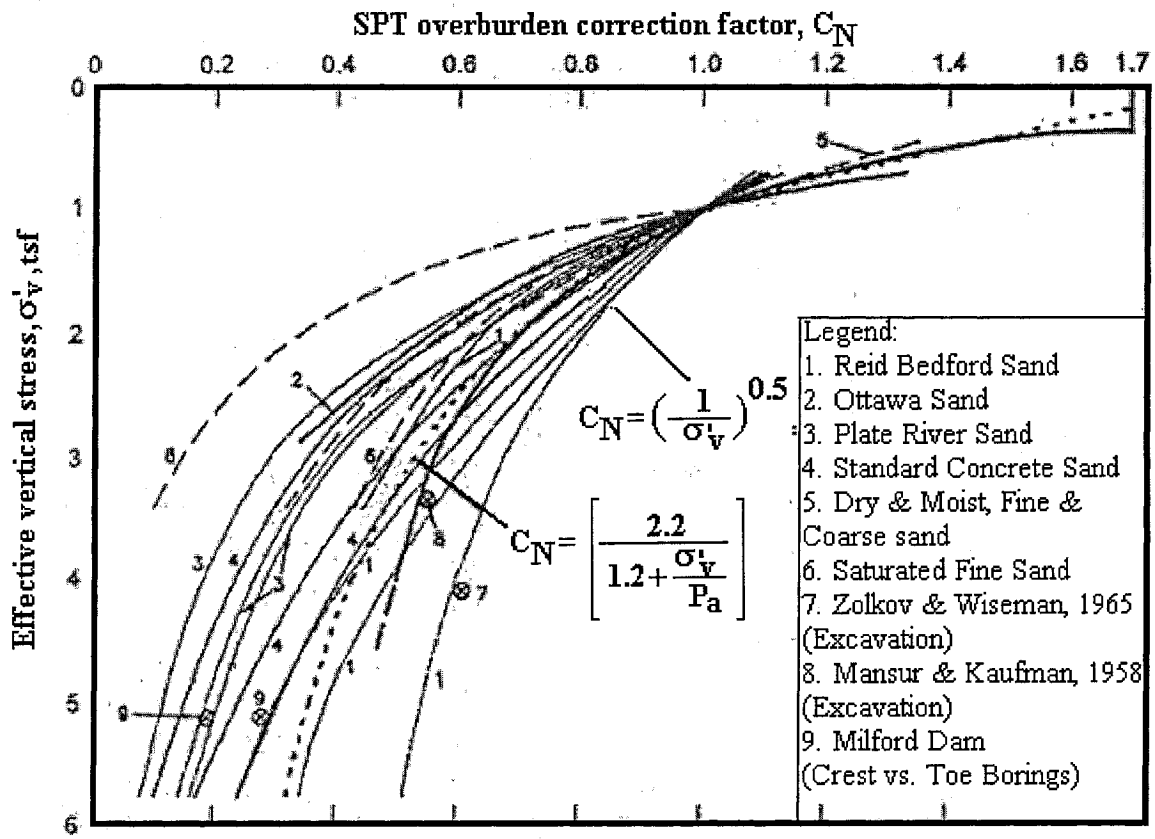

Figure 2.8: C_N Curves for various sands based on field and laboratory test data (Modified from Castro 1995 and published in Youd et. al. 2001)

Adjustment of cyclic resistance ratio, CRR, for the earthquake under consideration is done by magnitude scaling factor as given in Equation 2.8;

$$CRR = CRR_{7.5} x MSF \tag{2.8}$$

Where:

CRR = Cyclic resistance ratio adjusted for earthquake magnitude

$CRR_{7.5}$ = Cyclic resistance ratio for the magnitude 7.5 earthquakes specified by Seed and Idriss (1982),

MSF = Scale factor.

Various researchers including Ambraseys (1988), Arango (1996, Andrus and Stokoe (1997), Youd and Noble (1997) have proposed magnitude scaling factors given in Figure 2.9.

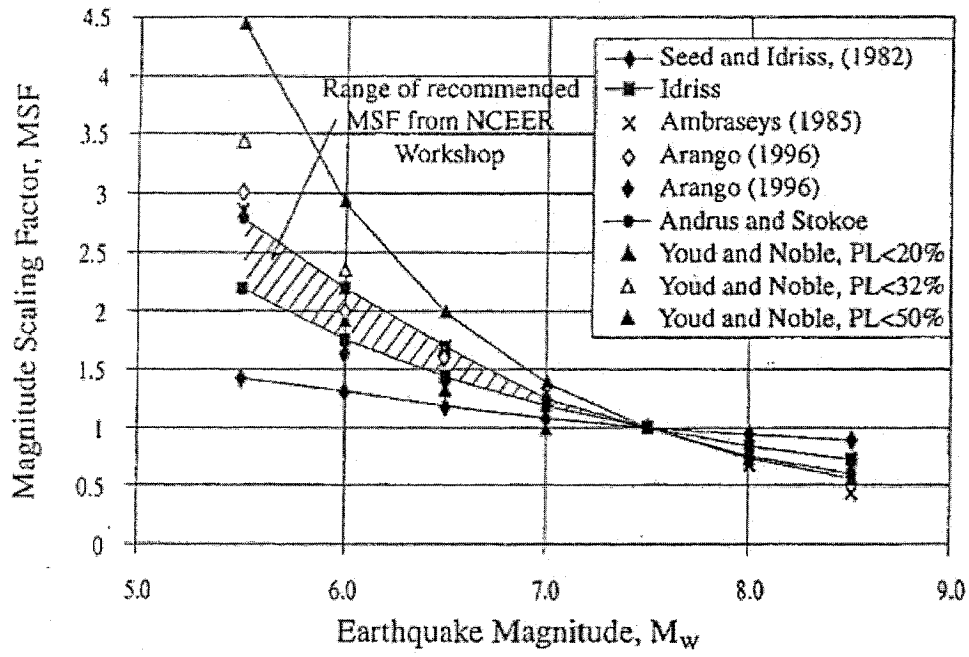

Figure 2.9: Magnitude scaling factors derived by various investigators

(Youd and Noble 1997)

2.3. LITERATURE REVIEW ON NEURAL NETWORK APPLICATIONS

Recently, ANN models were adopted by many researchers in the field of geotechnical engineering in solving varieties of problems. Goh (1995) developed a back propagation neural network, BPNN, model to assess soil liquefaction. He used eight soil and seismic parameters

including the standard penetration test value, mean grain size, fines content, equivalent dynamic shear stress, total and effective overburden stress, earthquake magnitude, and peak horizontal ground surface acceleration. He reported that neural networks were proven to be feasible tools for soil liquefaction assessments, simpler to apply and yield more reliable results when compared to conventional methodologies. It was noted that Goh (1995) has used relatively small dataset in developing the BPNN model, which considered the main limitation of ANN approaches. However, these models could be improved as new field case records become available.

In his second neural network model for soil liquefaction potential evaluation, Goh (1996) introduced a new field test parameter, which is the cone penetration resistance, to the model and removed SPT-N value parameter. The most important parameter was considered to be cone penetration resistance. He concluded that his approach was simpler as no calibration and/or normalization was required to reach reliable output. It was also concluded that the performance of neural network model could be improved as further field case records became available.

In his further study, Goh (2002) developed PNN models to analyze the databases based on cone penetration tests and shear wave velocity data. In this research, soil particle-size information was introduced as an input variable and the liquefaction phenomenon was considered as a classification problem.

Ural and Saka (1998) developed a BPNN model based on liquefaction records of earthquakes from Japan, China, North and South America. In this research, a small number of case records were used in the developing stage and the model was limited to sandy soil type.

Juang at. al. (1999) developed two BPNN models using model-based data and actual field results to compare Olsen and Robertson methods for liquefaction potential evaluations. The Robertson method reported to be slightly more accurate and conservative, although, both methods are fairly accurate in predicting liquefaction resistance of sandy soils.

Barai and Agarwal (2002) investigated Instance Based Learning, IBL, and models to assess soil liquefaction potential. The IBL model is tested on cone penetration test dataset and reported to yield better results when compared to existing regression models. As a final note, the authors suggested exploring hybrid model combining IBL and neural networks.

Juang et. al. (2003) trained a neural network model to develop a CPT-based empirical equation defining the unknown boundary curve, also known as limit state function. It is reported that their method compares favorably to widely used existing methods, is simpler in formulation, is easier to apply, and applicable to a wider range of soils.

Hanna et. al (2004) explored the efficiency of group piles in cohesionless soil using artificial neural networks. Utilizing a back propagation neural network model, pile group efficiency was addressed by introducing several governing parameters including the method of pile installation, soil condition, cap condition, type of loading, pile cross section, pile length/diameter ratio, pile spacing/diameter ratio, and pile arrangement. The outcome of the model provides correct prediction in more than 80 percent of the cases while the conventional methods provide correct prediction in 45 percent of the cases at maximum.

2.4 DISCUSSION

Based on the above literature review, it can be concluded that simplified methods are still under development and not sufficiently formulated for routine engineering practices. Also, it is evident that general consensus is not existed and it is not anticipated to occur in the near future. However, the rate of progress in soil liquefaction potential evaluation is impressive.

The purpose of this research is to make the best use of all the above-mentioned information and to build a neural network model that predicts the soil liquefaction potential in layered soils, in order to prevent human and property loss.

CHAPTER 3

ANALYSIS OF DATA

3.1 GENERAL

NCEER, 2000 and PEER 2001 and 2002 have collaboratively reported the laboratory and the field test results of the two earthquakes that took place in Chi-Chi, Taiwan (1999) and Kocaeli, Turkey in 1999. These records are used to develop the proposed soil liquefaction potential evaluation models. Given in Table 3.1 below, the field data includes 27 CPT profiles and 25 SPT borings from the 1999 Chi-Chi, Taiwan earthquake (magnitude M_v=7.6) region and 43 CPT profiles and 38 SPT borings from the 1999 Kocaeli, Turkey earthquake (magnitude M_v=7.4) region.

Table 3.1: Total number of in-situ tests used in this research

Field Tests	*Turkey Earthquake*	*Taiwan Earthquake*
Number of CPT Profiles	43	27
Number of SPT Borings	38	25
Total	81	52

3. 2 STANDARD PENETRATION TEST

Standardized in ASTM D1958, the SPT is one of the most popular and economical in-situ soil testing methods. The outcome of this test is the SPT blow count (N) numbers that are believed to be a good indicator of soil strength. In order to apply the SPT test, a hole is bored to a desired depth. Then, sampler is plugged to the tip of the drilling rod and derived into the bottom of the hole by means of a 63.5 kg hammer. The hammer is dropped freely from a height of 0.76

m. The sampler is first driven to a depth of 15 cm, then the hammer blow numbers required to drive the sampler to 30 cm are recorded. The reason for ignoring the first 15 cm is to reduce the effect of soil disturbance into experiment results. As a general rule, the penetration of the sampler should be halted if (i) 50 blows are required for any 15 cm increment, (ii) 100 blows are obtained, and (iii) 10 successive blows produced no advancement. The results are highly dependant on the care of the technicians on site. The schematic view of SPT application in the field is given in Figure 3.1

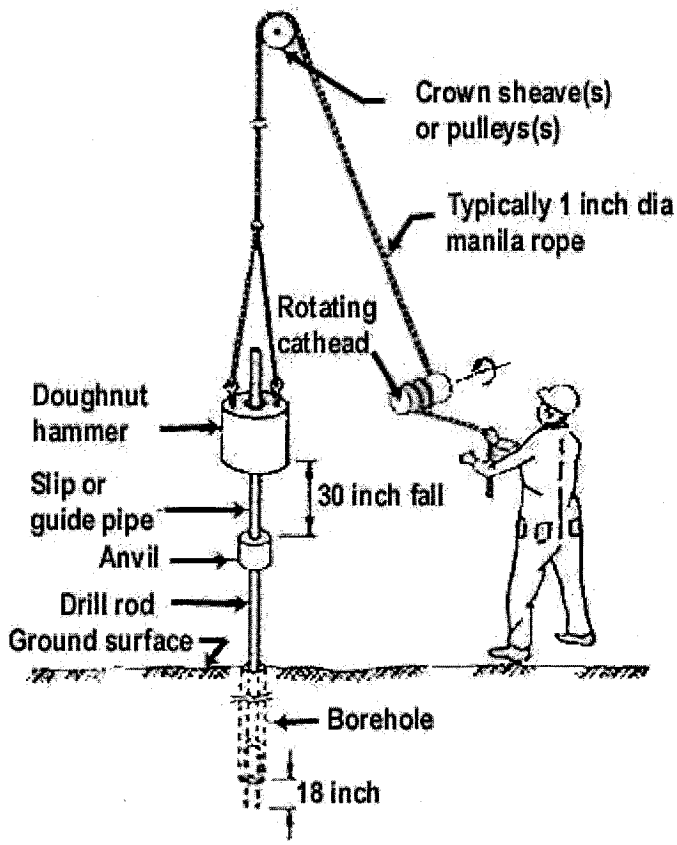

Figure 3.1: SPT application on site

In addition to SPT – N number, this test provides soil samples for visual description and/or laboratory tests. Undisturbed soil samples can be obtained from Shelby tube sampler, which is lowered into the soil at a constant rate. Soil specimens inside the tube are covered by wax to preserve their natural moisture content. On the other hand, split spoon sampler using is also a commonly practiced method of sample recovery.

3.3 CONE PENETRATION TEST

Standardized in ASTM D 3441-86, cone penetration test is used to identify soil type and stratification by means of nearly continuous readings of tip and skin resistance measurements. Commonly used penetrometers have 60° point angle and base diameters of 35,7 mm resulting in a projected area of 150 cm^2. The loading systems for penetrometers are often vehicles with enclosed cabins allowing in-situ testing under all weather conditions. The CPT steel probes are hydraulically penetrated inside the soil at a constant rate of 10 mm/s. In addition to cone tip resistance and sleeve friction, CPT measures friction ratio, which is the ratio between the local sleeve friction and cone resistance. Pore water pressure measurements are also possible in CPT testing. As shown in Figure 3.2, CPT penetrometers have standard geometric shapes.

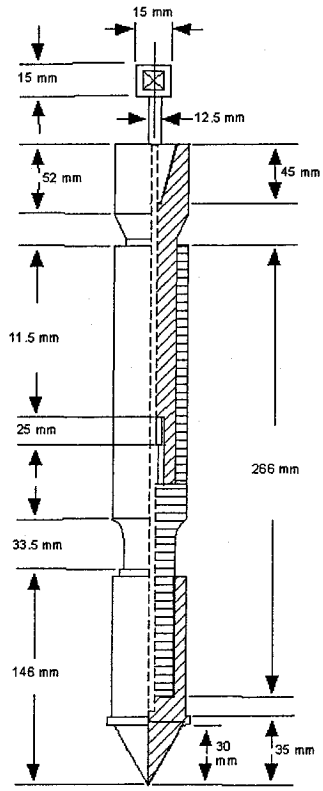

Figure 3.2: CPT Apparatus

3.4 SPT & CPT DATABASES

The proposed soil liquefaction potential models consist of two separate experimental datasets. One of the datasets is composed mostly of SPT parameters and the other is composed mostly of CPT parameters. Therefore, herein after the datasets will be referred to as **SPT database** and **CPT database**. A total of 620 case records were utilized for the SPT database, and 3895 case records were utilized for the CPT database. Given in Table 3.2 case histories are taken from liquefied and non-liquefied sites. As presented in Table 3.3, these case records were divided randomly into testing, training, and validation datasets.

Table 3.2: Distribution of the Data for liquefaction occurrence

Database	***Liquefied***	***Non-liquefied***	***Total Case Histories***
SPT Database	364	256	620
CPT Database	1665	2230	3895

Table 3.3: Distribution of the Data among Phases

Database	***SPT Database***			***CPT Database***		
Earthquake	*Turkey*	*Taiwan*	*Total*	*Turkey*	*Taiwan*	*Total*
Training	220	193	413	1360	1562	2922
Testing	59	53	112	239	282	521
Forecast	51	44	95	213	239	452
Total	330	290	620	1812	2083	3895

3.5 SOIL AND SEISMIC PARAMETERS

Soil and seismic parameters characterizing soil type and material properties, seismic attenuation characteristics, magnitude and nature of loads, and other site conditions including stress, strain, strength, saturation and seismological aspects were selected and incorporated into the databases. As shown in Table 3.4, twelve soil and seismic parameters were used for the SPT database.

Table 3.4: SPT parameters used in the database

SPT Database Parameters	***Abbreviations***	***Unit***
Depth of soil specimen	z	m
Corrected SPT blowcount	$(N_1)_{60}$	-
Percent fines content less than 75 mm	F≤75 μm	%
Depth of ground water table	d_w	m
Total overburden stress	σ_{vo}	kPa
Effective overburden stress	σ'_{vo}	kPa
Threshold acceleration	a_t	g
Cyclic stress ratio	τ_{av}/σ'_{vo}	-
Shear wave velocity	V_s	m/s
Internal friction angle of soil	ϕ'	o
Earthquake magnitude	M_v	-
Maximum horizontal acceleration at ground surface	a_{max}	g

Given in Table 3.5, twelve soil and seismic parameters are used for CPT database.

Table 3.5: CPT parameters used in the database

CPT Database Parameters	***Abbreviations***	***Unit***
Depth of soil specimen	Z	m
Total overburden stress	σ_{vo}	kPa
Effective overburden stress	σ'_{vo}	kPa
Depth of ground water table	d_w	m
CPT cone tip resistance	q_c	kPa
CPT sleeve friction resistance	f_s	kPa
CPT friction ratio	R_f	-
Shear wave velocity	V_s	m/s
Threshold acceleration	a_t/g	g
Cyclic stress ratio	τ_{av}/σ'_{vo}	-
Earthquake magnitude	M_v	-
Maximum horizontal acceleration at ground surface	a_{max}	g

3.6 DATABASE DEVELOPMENT PROCEDURE

Databases are developed according to the procedure introduced by Youd. et. al. (2001), Seed et. al. (2003), and other backbone studies mentioned in the literature review section. The details of the development procedure are given in the following sections of this chapter.

3.6.1 SPT DATABASE

In the SPT database, maximum horizontal acceleration at ground surface values, earthquake magnitude, depth of the soil samples, SPT – N values, fines contents, shear wave velocities and ground water table elevations are the actual measured values. The remaining design parameters were obtained by related correlations as described below.

In Table 3.11, the depths of the soil specimen, given in the first column, is taken up to 20m from the ground surface because the simplified method was developed and applicable for shallow depths. The standard penetration test results, given in column 2, were corrected according to the Equation 3.1, which was described by Youd et al. (2001) below;

$$(N_1)_{60} = N_m C_N C_R C_S C_B C_E \tag{3.1}$$

Where,

$(N_1)_{60}$ = Corrected SPT blowcount

N_m = Measured SPT penetration resistance

C_N = Correction to normalize SPT blowcount to a common reference effective overburden stress

C_R = Correction factor for borehole diameter

C_S = Correction factor for non-standardized sampler configuration

C_B = Correction factor for borehole diameter

C_E = Correction factor for hammer energy efficiency

Named also as the overburden stress correction factor, the normalization factor (C_N) corrects the SPT penetration resistance to an equivalent value under one atmosphere of effective overburden stress by the following Equation 3.2 given by Liao and Whitman (1986a);

$$C_N = \left(\frac{P_a}{\sigma'_{vo}}\right)^{0.5} \leq 1.7 \tag{3.2}$$

Where:

P_a = Atmosphere pressure (1 atm=101,325 kPa)

σ'_{vo} = Effective overburden pressure

The correction to normalize the SPT blowcount to a common reference effective overburden stress (C_N) should not exceed a value of 1.7. This value represents the consensus reached after National Center for Earthquake Engineering Research (NCEER) working group (NCEER 1997, Youd et. al.2001).

The range of the other correction factors indicated in Equation 3.1 is given in Table 3.6 below.

Table 3.6: Corrections to SPT (Modified from Skempton 1986)

as listed by Roberts and Wride (1998)

Factor	Equipment variable	Term	Correction
Overburden pressure	-	C_N	$(P_a/\sigma'_{vo})^{0.5}$
Overburden pressure	-	C_N	$C_N \leq 1.7$
Energy ratio	Donut hammer	C_E	0.5-1.0
Energy ratio	Safety hammer	C_E	0.7-1.2
Energy ratio	Automatic-trip- Donut-type hammer	C_E	0.8-1.3
Borehole diameter	65-115 mm	C_B	1.0
Borehole diameter	150 mm	C_B	1.05
Borehole diameter	200 mm	C_B	1.15
Rod length	<3 m	C_R	0.75
Rod length	3-4 m	C_R	0.8
Rod length	4-6 m	C_R	0.85
Rod length	6-10 m	C_R	0.95
Rod length	10-30 m	C_R	1.0
Sampling method	Standard sampler	C_S	1.0
Sampling method	Sampler without lines	C_S	1.1-1.3

Regarding correction factor for hammer energy efficiency, the Equation 3.3 is used in calculations;

$$C_E = \frac{ER}{60\%} \tag{3.3}$$

Where:

ER = hammer efficiency ratio

Hammer efficiency ratios (ER) for Kocaeli earthquake case records are the actual values measured in the field. However, the "ER" values for Taiwan earthquake case records were based on strain gauge measurements due to failing accelerometers. Therefore, the "ER" values reported by Stewart et al. (2001) were adjusted to 69% for depths up to 3m and 75% for depths below 3m. The field energy measurements during SPT testing in the Taiwan earthquake region are given in Figure 3.3 below.

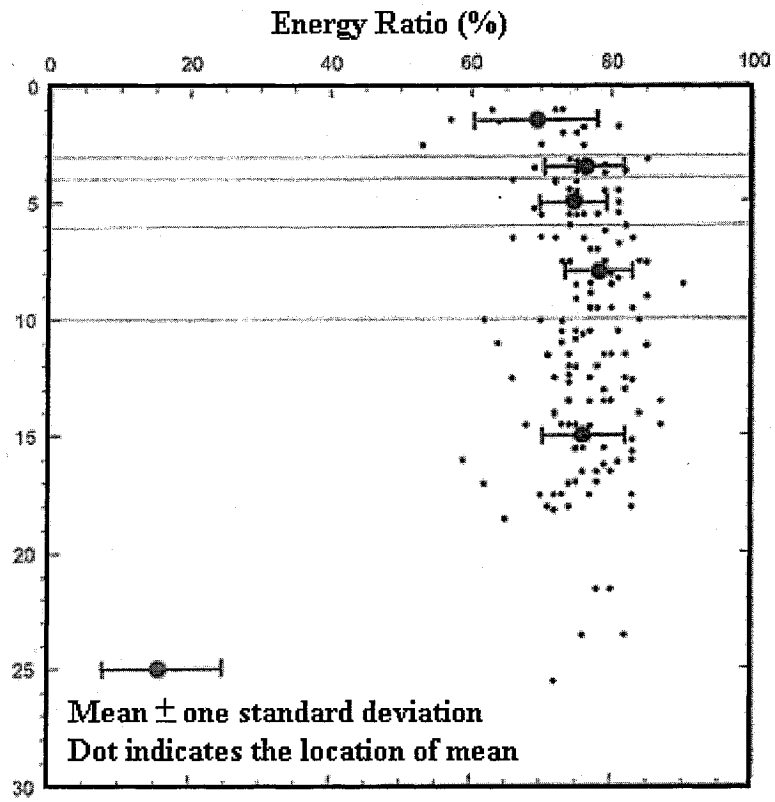

Figure 3.3: Field energy ratio measurement during SPT testing

in Taiwan Earthquake region (Stewart et. al. 2001)

Additionally, in order to approximate the corrected SPT blow counts; the finest content (FC) influence is taken into consideration by utilizing the equations given below (Youd et. al. 2001);

$$(N_1)_{60,cs} = \alpha + \beta(N_1)_{60} \tag{3.4}$$

Where:

α and β = Coefficients determined from the following Equations 3.5 & 3.6, respectively;

$$\alpha = 0 \qquad \text{for FC} \leq 5\% \tag{3.5a}$$

$$\alpha = \exp[1.76 - (190/FC^2)] \qquad \text{for } 5 \leq \text{FC} \leq 5\% \tag{3.5b}$$

$$\alpha = 5.0 \qquad \text{for FC} \geq 35 \tag{3.5c}$$

And

$$\beta = 1.0 \qquad \text{for FC} \leq 5\% \tag{3.6a}$$

$$\beta = [0.99 - (FC^{1.5}/1000)] \qquad \text{for } 5 \leq \text{FC} \leq 5\% \tag{3.6b}$$

$$\beta = 1.2 \qquad \text{for FC} \geq 35\% \tag{3.6c}$$

In Table 3.11, column 3 presents the percentage finest content less than 75 μm, which are the actual values measured in the field. Finest content is also taken into consideration while calculating the cyclic resistance ratio ($CRR_{7.5}$), due to its notable influence on soil liquefaction (Seed et. al. 1985). The depth of the ground water table is given in column 4 in Table 3.11. Total and effective overburden stresses are presented in column 5-6 respectively.

Being a strain problem, SPT liquefaction database includes threshold acceleration values listed in column 7 of the Table 3.11. Threshold acceleration values are obtained by the procedure given by Dobry et. al. (1981;1982) and Zengal et. al. (1994) and defined as the Equation 3.7 below;

$$\frac{a_t}{g} = \frac{V_s^2 \cdot \left(\frac{G}{G_{\max}}\right)_t \cdot \gamma_t}{g.z.r_d.(0.1(M-1))} \tag{3.7}$$

Where:

V_s = Shear wave velocity

γ_t = Threshold strain

$(G/G_{max})_t$ = Modulus reduction factor at the threshold

r_d = Stress reduction coefficient (See Equation 3.9)

M = Magnitude of the earthquake

g = Acceleration of gravity

In this relation, with the strain level of order of 0.01% the modulus reduction factor at the threshold is assumed to be 0.8 (Hardin et. al. 1972). The relationship between the shear modulus and the shear strain is given in Figure 3.4;

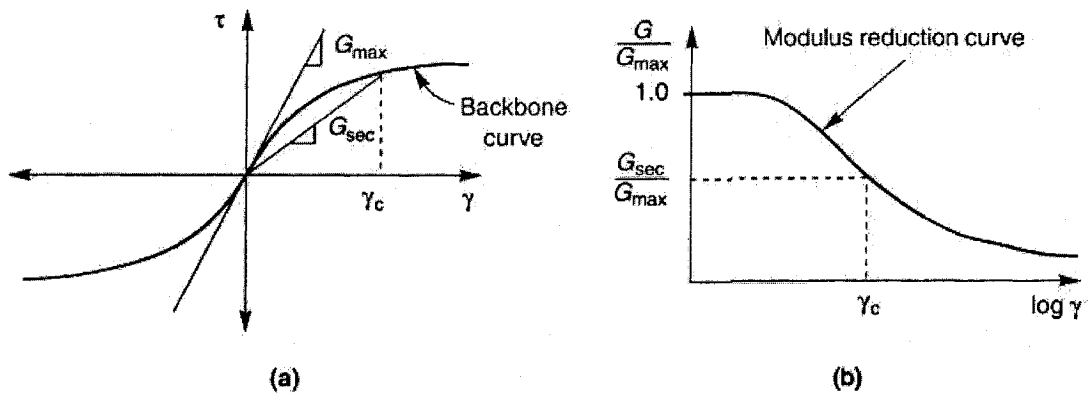

Figure 3.4: Relationship between the shear modulus and the shear strain

In column 8 of the Table 3.11, cyclic stress ratios required to generate soil liquefaction were tabulated. Existing correlations formulated by Seed and Idriss (1971) allows the cyclic stress ratio, CSR, to be defined as:

$$CSR = \frac{\tau_{av}}{\sigma'_{vo}} = 0.65(\frac{a_{max}}{g})(\frac{\sigma_{vo}}{\sigma'_{vo}})r_d \quad (3.8)$$

Where,

a_{max} = Peak horizontal acceleration at the ground surface generated by the earthquake

g = Acceleration of gravity

σ_{vo} = Total overburden stress

σ'_{vo} = Effective overburden stress

r_d = Stress reduction coefficient

Stress reduction coefficient, r_d, is calculated by Equation 3.9 which is the approximation of the mean curve plotted in Figure 3.5;

$$r_d = \frac{1.00 - 0.4113z^{0.5} + 0.04052z + 0.001753z^{1.5}}{1.00 - 0.4177z^{0.5} + 0.05729z - 0.006205z^{1.5} + 0.001210z^2} \tag{3.9}$$

Where,

z = Depth of soil beneath ground surface.

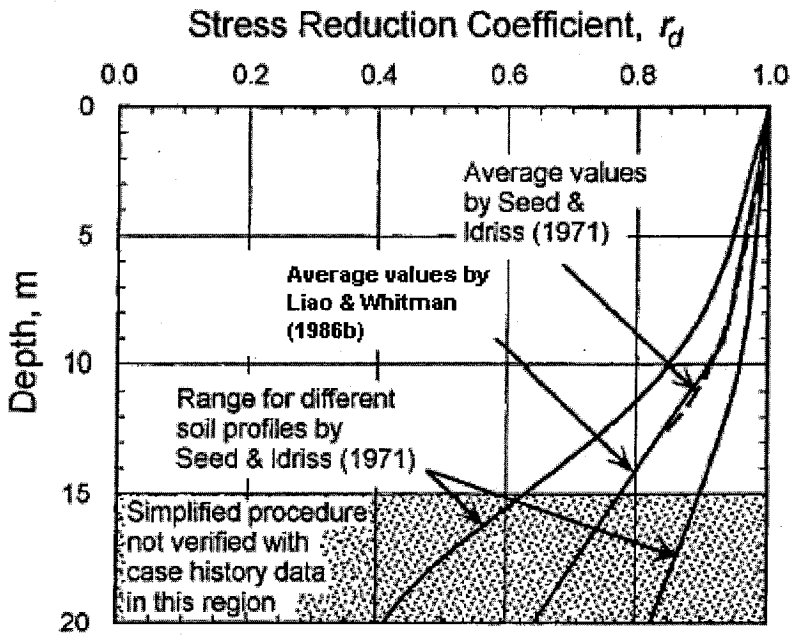

Figure 3.5: r_d versus Depth Curves Developed by Seed and Idriss (1971) and Liao and Whitman (1986b) (Published in Youd et. al. 2001)

In column 9 of Table 3.11, the shear wave velocities, which were the actual measured values from related seismic cone test (SCPT) and spectral analysis of surface waves test (SASW) were presented.

The angle at which soil resists shearing is defined as the internal friction angle and it is tabulated in column 10 of the Table 3.11. The relative density influences the shear strength of sands and consistency influences the shear strength of clays. From the empirical correlation between internal friction angle (ϕ') and plasticity index (PI) given in Figure 3.6, internal friction angle for clay soils are evaluated by the following equation:

$$\sin\phi' = -0.229\log_{10} PI + 0.807 \tag{3.10}$$

Where:

PI = Plasticity Index (%)

ϕ' = Internal friction angle

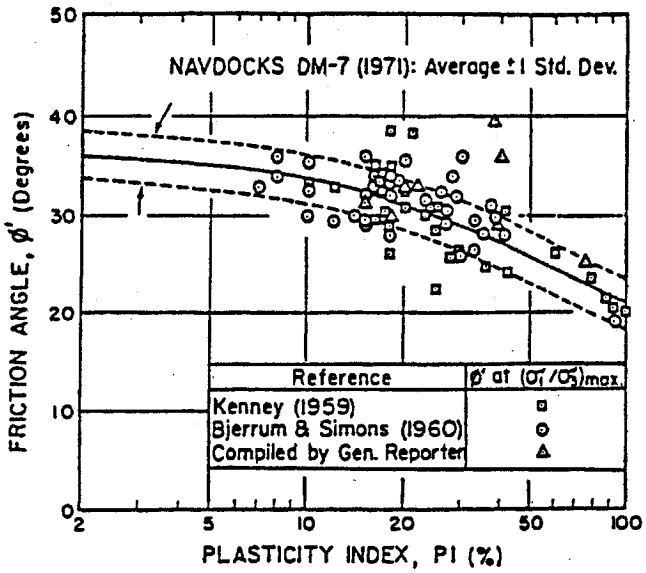

Figure 3.6: Empirical correlation between friction angle and plasticity index from triaxial compression tests on normally consolidated undisturbed clays (JSSMFE 1988).

Terzaghi & Peck (1967) proposed the values of friction angle for sands and silts given in Table 3.7

Table 3.7: Representative values of ϕ' for sands and silts. (Terzaghi and Peck 1967)

Material	*Degrees*	
	Loose	*Dense*
Sand, round grains, uniform	27.5	34
Sand, angular grains, well graded	33	45
Sandy gravels	35	50
Silty sands	27-33	30-34
Organic silts	27-30	30-35

Dunhum (1954) proposed the correlation between friction angle and N-value, and proposed the following Table 3.8. By using the definitions of the layers in the data set, a consistent equation is chosen.

Table 3.8: Internal friction angle relations based on shape classification (Dunhum 1954).

Group Name	***ϕ Relation***
For ground grains of uniform size	$\phi=(12N)^{1/2}+15$
For ground grains, well graded	$\phi=(12N)^{1/2}+20$
For sharp grains of uniform size	$\phi=(12N)^{1/2}+20$
For sharp grains, well graded	$\phi=(12N)^{1/2}+25$

As depicted in the Figure 3.7, a correlation between N-value and ϕ' is given, in addition to studies of Terzaghi and Peck (1948, 1967) and Dunhum (1954). Studies of Kolb & Shockly (1957) regarding intervals of internal friction angle for clays, silts and sands are given in Table 3.9 below.

Table 3.9: Intervals of internal friction angle for clays, silts and sands (Kolb & Shockly 1957)

Predominant Soil Texture	***Angle of friction (°)***
Clay sands (SC) to silty clays(CL)	30
Sands (SP)	30-40
Silts (ML) and silty sands (SM)	25-35
Sands (SP)	30-38
Clay silts and silty clays (CL and CH)	15-20
Silts (ML)	10-35

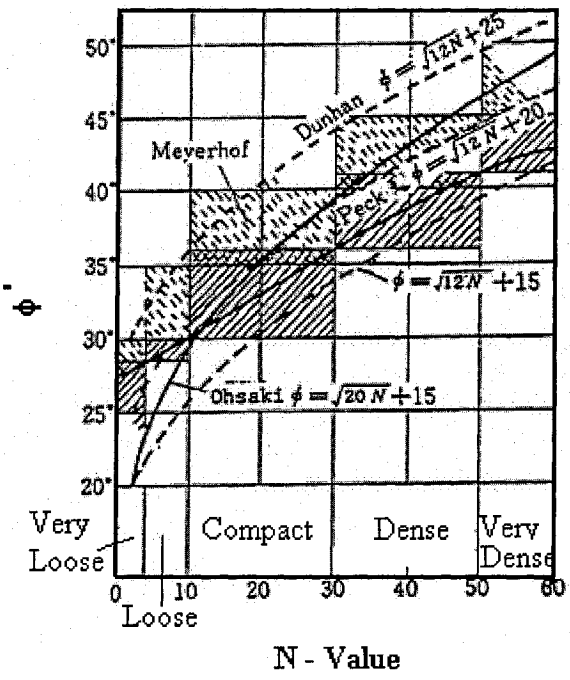

Figure 3.7: Comparison of the correlation between N-value and ϕ' (JSSMFE 1988)

Earthquake magnitudes of all the soil data obtained from Turkey and Taiwan earthquake regions are given in column 11 of Table 3.11. Maximum horizontal accelerations at ground surface are given in the column 12. The distribution of the peak accelerations recorded by strong motion station is given in Table 3.10 below.

Table 3.10: Maximum horizontal accelerations recorded by strong motion stations

Area	***Taiwan***			***Turkey***
Location	Nantou	Wufeng	Yuanlin	Adapazari City
Value	0.38 (g)	0.67 (g)	0.18 (g)	0.4 (g)
Station	TCU076	TCU065	TCU110	NSMP*

* National Strong Motion Network

This study explores the liquefaction potential of layered soils. It is not possible however, to investigate liquefaction potential of soil strata at particular depth by field observations. Thus, conventional methods are used to calculate the possibility of liquefaction at each depth. SPT test results supported by shear wave velocity measurements are capable of accurately identifying and predicting liquefaction potential of liquefiable layers. Accordingly, the liquefaction potential of soil layers has been evaluated by means of an assortment of empirical criteria, which was sometimes found to be more reliable than analytical calculations and frozen sampling. Given in column 13 in Table 2 above, liquefaction susceptibility of soils in Turkey and Taiwan earthquake regions are determined by the three following criteria (i) stress-based liquefaction triggering analyses developed for SPT tests (Youd et. al. 2001) (ii) strain-based procedure (Dobry et. al. 1982), and (iii) Chinese criteria (Finn (1991) and Finn et. al. 1994).

Formulized in Equation 3.11, the soil layer at the depth of the measured SPT is regarded as liquefied if $FS_{liq} \leq 1.0$, while $FS_{liq} > 1.0$ indicates no liquefaction. (Ishihara 1985, 1993; Seed and Harder 1990)

$$FS_{liq} = (\frac{CRR_{7.5}}{CSR})MSF \tag{3.11}$$

Where,

CSR = Cyclic stress ratio given by Seed and Idriss (1971),

$CRR_{7.5}$ = Cyclic resistance ratio for the magnitude 7.5 earthquakes specified by Seed and Idriss (1982),

MSF = Scale factor.

$CRR_{7.5}$ is determined from the results of the SPT (N values). The $CRR_{7.5}$ curve is given in Figure 3.8 below. The CRR curve for fines content <5% is referred to as "SPT clean sand base curve".

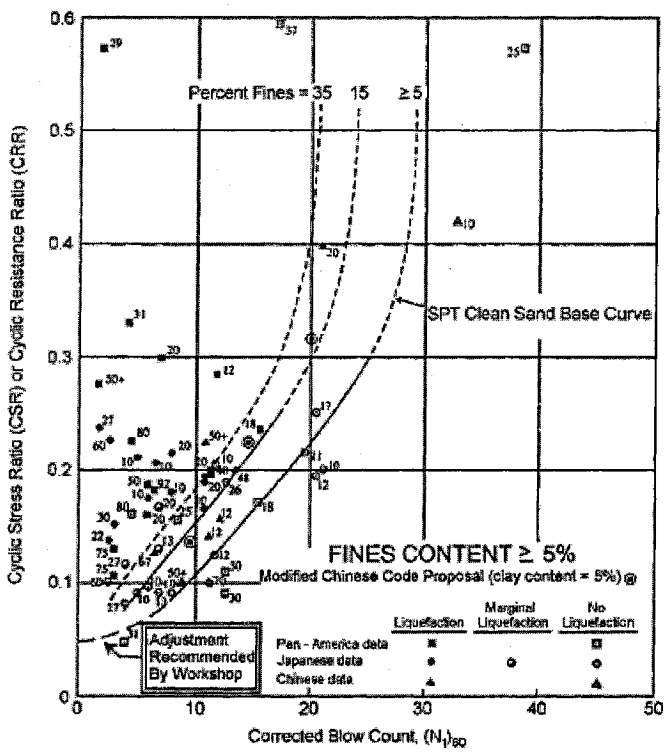

Figure 3.8: SPT Clean-Sand Base Curve for Magnitude 7.5 Earthquakes with Data from Liquefaction Case Histories (Youd et. al. 2001)

Clean sand base curve is approximated and defined as the Equation 3.12 (Youd et. al. 2001). In application, $(N_1)_{60,cs}$ values should be used in this equation;

$$CRR_{7.5} = \frac{1}{34-(N_1)_{60}} + \frac{(N_1)_{60}}{135} + \frac{50}{(10(N_1)_{60}+45)^2} - \frac{1}{200} \qquad (3.12)$$

Clean granular soil exceeding $(N_1)_{60} \geq 30$ are regarded as too dense to liquefy, therefore the equation is valid for only $(N_1)_{60} < 30$.

The earthquakes utilized in this paper have magnitudes of 7.4 for Kocaeli/ Turkey earthquake and 7.6 for Taiwan earthquake. These magnitudes call for magnitude scaling due to the fact that aforementioned $CRR_{7.5}$ approximations are based on certain magnitude of 7.5. Andrus and Stokoe (1997) studied earthquakes with different magnitudes and they developed bounding curves for their studies of liquefaction resistance. By taking the ratio of CRR for a given magnitude to the $CRR_{7.5}$, magnitude-scaling factors are generated and given by the Equation 3.13.

$$MSF = (M_w / 7.5)^{-3.3} \tag{3.13}$$

Where:

M_v = Magnitude of the earthquake

Seed et. al. (1985) correlation, modified by Youd et .al. (2001), is controlled by mostly clean sands and silty sands with less than 35% fines; however, many of case histories from both earthquake regions involve high cyclic stress ratios and high finest content soils. Therefore, three different soil liquefaction potential evaluation procedures are used. From an earthquake geotechnical engineer's point of view, these earthquakes provide an exceptional opportunity to advance the development of empirical liquefaction assessment methodology in that case histories in the city of Adapazari (Turkey) and the cities of Wufeng, Nantou and Yuanlin (Taiwan)

(Stewart et. al. 2003; Bray et. al 2002) and complete the necessary parameter spaces in the well known Seed et. al. (1985) procedure.

Based on the Youd et. al. (2001), the relationship between cyclic stress ratio and corrected standard penetration resistance for sands and silty sands with varying peak ground acceleration and earthquake magnitudes are given in Figure 3.9, 3.10, 3.11 and 3.12 below;

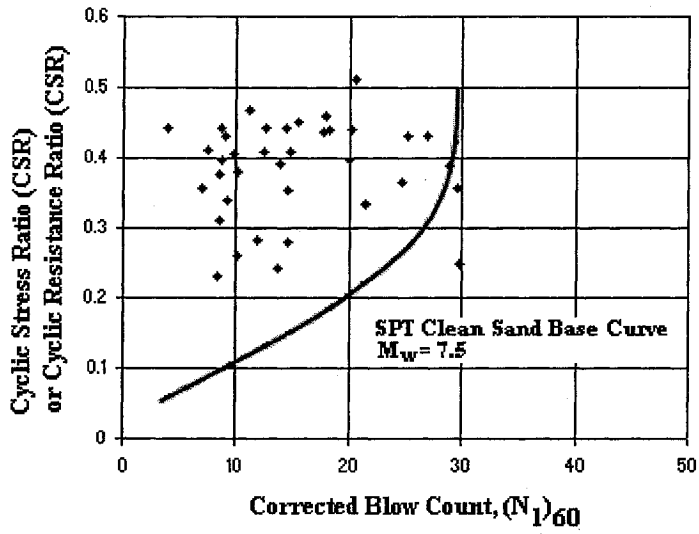

Figure 3.9: Relationship between cyclic stress ratio (CSR) and corrected standard penetration test (SPT) number for Kocaeli, Turkey Earthquake data for the peak ground acceleration (a_{max}) of 0.4 g and a moment magnitude (M_w) of 7.4 (Modified for the magnitude scaling factor given by Andrus and Stokoe 1997)

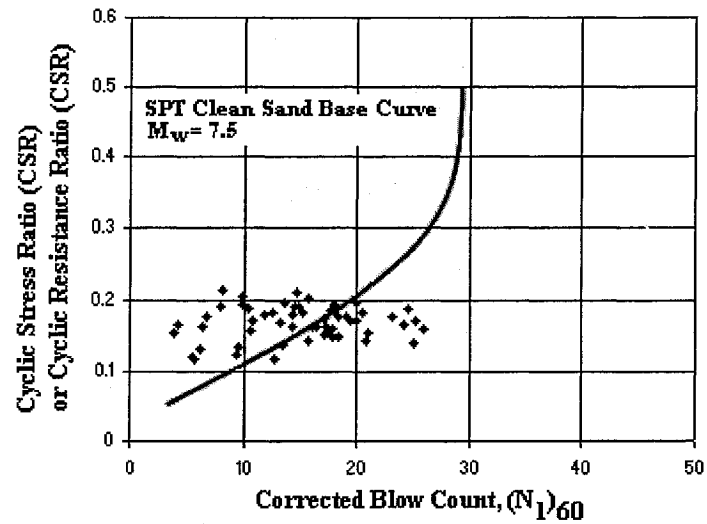

Figure 3.10: Relationship between cyclic stress ratio (CSR) and corrected standard penetration test (SPT) number for Chi-Chi, Taiwan Earthquake data for the peak ground acceleration (a_{max}) of 0.18 g and a moment magnitude (M_w) of 7.6. (Modified for the magnitude scaling factor given by Andrus and Stokoe 1997)

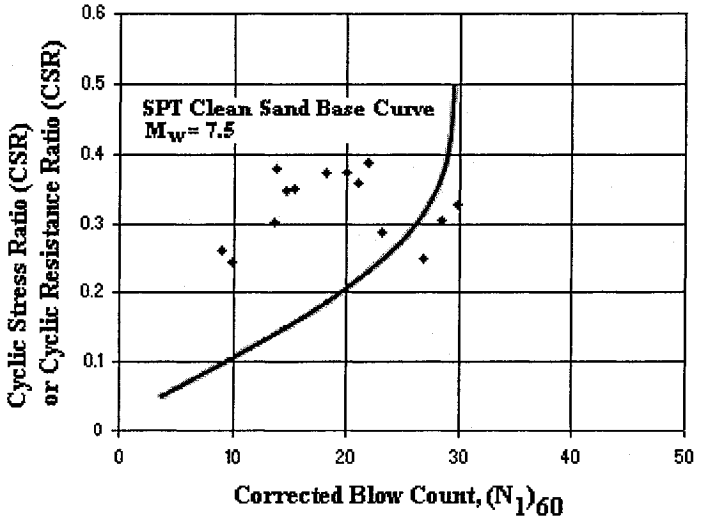

Figure 3.11: Relationship between cyclic stress ratio (CSR) and corrected standard penetration test (SPT) number for Chi-Chi, Taiwan Earthquake data for the peak ground acceleration (a_{max})

of 0.38 g and a moment magnitude (M_w) of 7.6. (Modified for the magnitude scaling factor given by Andrus and Stokoe 1997)

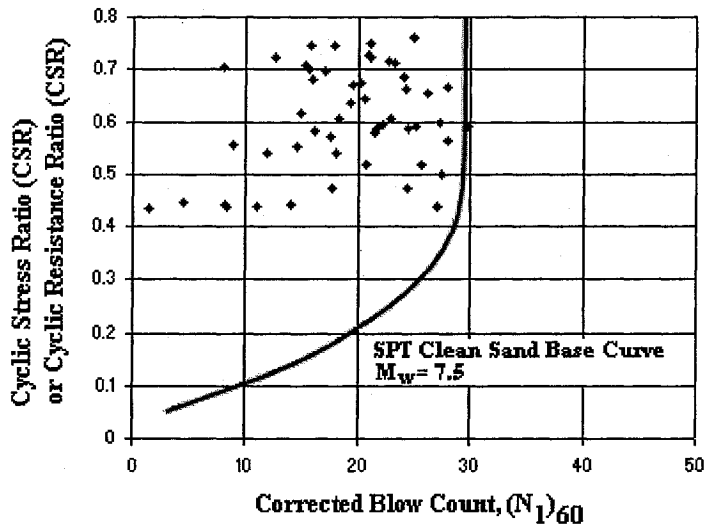

Figure 3.12. Relationship between cyclic stress ratio (CSR) and corrected standard penetration test (SPT) number for Chi-Chi, Taiwan Earthquake data for the peak ground acceleration (a_{max}) of 0.67 g and a moment magnitude (M_w) of 7.6. (Modified for the magnitude scaling factor given by Andrus and Stokoe 1997)

Regarding soils with plastic fines, Finn (1991) and Finn et. al. (1994) proposed modifications to "Modified Chinese Method". The evaluation of the liquefaction potential of soils with plastic fine is performed according to this procedure. If the soil index properties fall within the below-mentioned bounds, soil with plastic fines is considered vulnerable against loss of strength induced by soil liquefaction. These bounds are;

- Percent finer less than 0.005 mm $\leq$ 20%
- (Liquid limit + 1%) $\leq$ 35%

- (Water content + 2%) ≥ 0.9 x (Liquid limit + 1%)
- Liquidity index (based on Liquid Limit + 1% and water content + 2%) ≤ 0.75

The graphical representation of this criterion with soil data from both earthquakes is shown in Figures 3.13, 3.14, and 3.15.

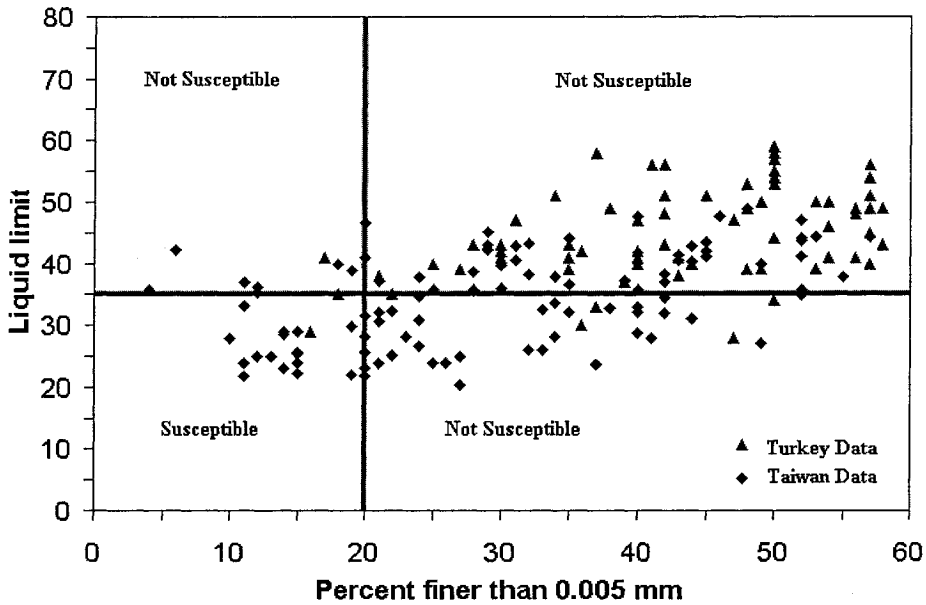

Figure 3.13. The distribution of liquid limit versus percent finer than 0.005 mm for both Turkey and Taiwan Earthquakes data

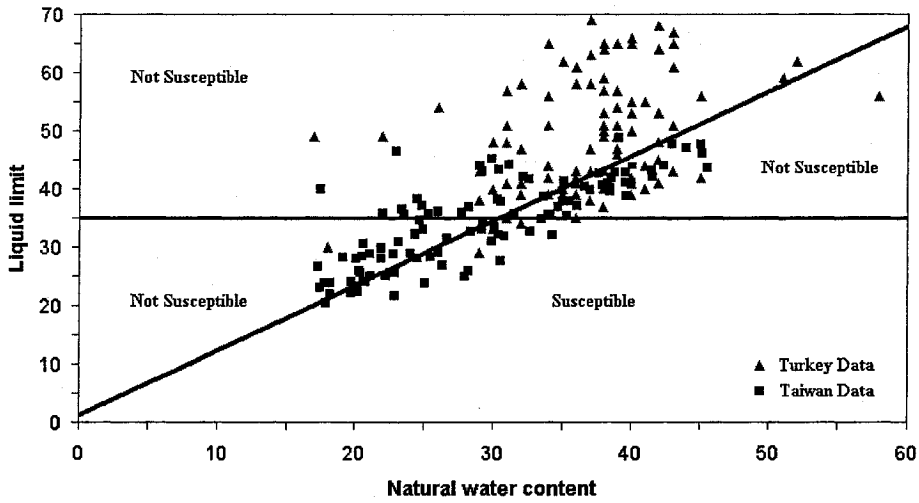

Figure 3.14. The distribution of liquid limit versus natural water content for both Turkey and Taiwan Earthquakes data

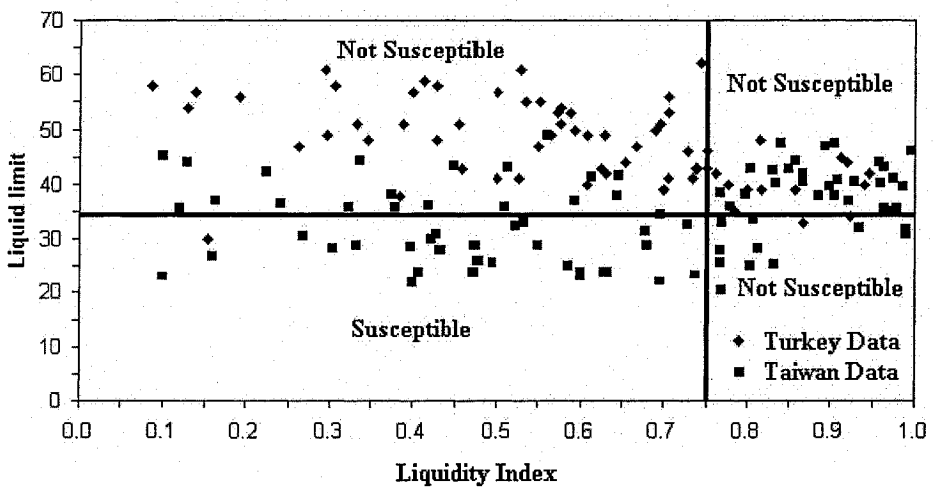

Figure 3.15: The distribution of liquid limit versus liquidity index for both Turkey and Taiwan Earthquake data

Given in Equation 3.14, the threshold acceleration can be calculated as follows;

$$\frac{a_t}{g} = \frac{V_s^2 \cdot \left(\frac{G}{G_{\max}}\right)_t \cdot \gamma_t}{0.65.g.z.r_d} \tag{3.14}$$

Where;

V_s = shear wave velocity

γ_t = threshold strain

$(G/G_{max})_t$ = modulus reduction factor at the threshold

r_d = stress reduction coefficient

M = magnitude of the earthquake.

The modulus reduction factor at the threshold, $(G/G_{max})_t$, was assumed to be 0.8 with a strain level of an order of 0.01% (Hardin et. al. 1972). Factor of safety in threshold acceleration criteria is given in Equation 3.15 below;

$$F_a = \frac{a_t}{a_{\max}} \tag{3.15}$$

$F_a > 1$ implies that there is no risk, $F_a \leq 1$ does not necessarily mean that liquefaction will occur; instead, the value predicts that there will be gross sliding of the grain-to-grain contact surfaces which is essential for excess pore water pressure generation and therefore crucial for liquefaction (Rauch 1997).

Table 3.11: Summary of SPT liquefaction case records

#	*1*	*2*	*3*	*4*	*5*	*6*	*7*	*8*	*9*	*10*	*11*	*12*	*13*
Parameters	**Z**	**$(N_1)_{60}$**	**F≤ 75μm**	**d_w**	**σ_{vo}**	**σ'_{vo}**	**a_t**	**τ_{av}/σ'_{vo}**	**V_s**	**ϕ'**	**M_v**	**a_{max}**	**Liquefaction**
Unit	**(m)**	**-**	**(%)**	**(m)**	**(kPa)**	**(kPa)**	**(g)**	**–**	**(m/s)**	**(°)**	**-**	**(g)**	**-**
Summary of testing phase	4.2	5	74	0.77	75.8	41.5	0.02	0.44	85	26.93	7.4	0.40	yes
	6.0	4	99	0.78	109.5	57.3	0.15	0.45	250	29.97	7.4	0.40	no
	4.6	22	4	2.28	80.6	57.4	0.06	0.33	145	40.10	7.4	0.40	yes
	4.2	6	19	2.30	64.4	45.7	0.09	0.16	167	26.93	7.6	0.18	yes
	11.8	8	66	2.30	203.1	110.0	0.03	0.19	159	29.17	7.6	0.18	Yes
	17.2	30	20	0.99	339.1	180.0	0.10	0.33	315	39.29	7.6	0.38	no
	10.2	18	38	0.70	237.1	143.9	0.05	0.37	188	34.28	7.6	0.38	yes
Summary of training phase	1.8	8	94	0.77	30.9	20.6	0.08	0.37	105	29.17	7.4	0.40	no
	1.0	3	74	0.78	18.0	15.8	0.14	0.29	105	26.00	7.4	0.40	yes
	3.4	2	85	0.78	62.4	36.2	0.03	0.42	85	29.14	7.4	0.40	no
	4.2	6	97	2.50	72.5	55.9	0.07	0.15	150	32.44	7.6	0.18	no
	16.2	30	91	1.90	332.1	191.8	0.13	0.31	363	39.60	7.6	0.38	no
	1.8	4	98	1.14	29.7	23.2	0.30	0.56	208	24.90	7.6	0.67	yes
	12.2	36	32	1.14	238.2	129.7	0.07	0.69	239	39.60	7.6	0.67	no
Summary of validation phase	7.0	31	3	1.68	138.2	85.0	0.33	0.37	400	43.97	7.4	0.40	no
	7.3	9	99	1.72	133.2	77.4	0.01	0.39	81	29.80	7.4	0.40	no
	2.2	9	15	2.00	39.1	37.1	0.13	0.12	150	28.49	7.6	0.18	yes
	2.2	7	59	1.10	36.4	25.7	0.08	0.17	118	26.93	7.6	0.18	yes
	3.2	15	10	0.70	84.1	59.6	0.05	0.35	113	30.95	7.6	0.38	yes
	14.2	36	19	0.70	320.6	188.2	0.06	0.34	242	41.35	7.6	0.38	no
	3.8	18	20	3.20	64.6	58.7	0.10	0.47	167	32.00	7.6	0.67	yes
	16.2	13	72	0.50	334.1	180.1	0.06	0.59	250	36.97	7.6	0.67	no

3.6.2 CPT DATABASE

In CPT database, CPT tip resistance, CPT sleeve friction resistance, CPT friction ratio, maximum horizontal acceleration at ground surface values, earthquake magnitude, depth of the soil samples, shear wave velocities and ground water table elevations are the actual measured values. The remaining parameters were obtained by related correlations as described in (3.4.1 SPT Database Section).

In Table 3.12, depths of soil specimen in the first column were taken up to 20 meters from the ground surface. Total and effective vertical stresses are presented in column 2-3 respectively. The depth of ground water table is given in column 4. In Table 3.12, CPT test outcomes namely, cone tip resistance, sleeve friction resistance, and friction ratio values are presented in columns 5, 6 and 7 respectively. In column 8, the shear wave velocities, which were actual measured values form related seismic cone test (SCPT) and spectral analysis of surface wave test (SASW) were presented. The threshold acceleration values were calculated following the procedure given by Dobry et. al. (1981, 1982) and Zengal et. al. (1994) and given in column 9. The modulus reduction factor at the threshold, $(G/G_{max})t$ is assumed to be 0.8 with a strain level of an order of 0.01% (Hardin et. al. 1972).

In column 10 of Table 3.12, cyclic stress ratios required to generate soil liquefaction were tabulated (Seed and Idriss 1971). Column 11, presents the moment magnitude of the Turkey and Taiwan earthquakes, in which soil data obtained. Maximum horizontal accelerations at ground surface are given in column 12. The distribution of the peak accelerations recorded by strong motion station is given in Table 3.10.

Table 3.12: Summary of CPT liquefaction case records

#	*1*	*2*	*3*	*4*	*5*	*6*	*7*	*8*	*9*	*10*	*11*	*12*	*13*
Parameters	**Z**	**σ_{vo}**	**σ'_{vo}**	**d_w**	**q_c**	**f_s**	**R_f**	**V_s**	**a_t**	**τ_{av}/σ'_{vo}**	**M_v**	**a_{max}**	**Liquefaction**
Unit	**(m)**	**(kPa)**	**(kPa)**	**(m)**	**(kPa)**	**(kPa)**	**(-)**	**(m/s)**	**(g)**	**(-)**	**(-)**	**(g)**	**(-)**
Summary of testing phase	3.6	66.1	37.9	0.78	577.5	6.1	1.06	85	0.027	0.422	7.4	0.40	no
	6.8	122.8	62.4	0.77	1207.5	35.6	2.95	173	0.062	0.452	7.4	0.40	yes
	4.8	88.2	53.5	1.34	739.9	24.3	3.28	85	0.021	0.392	7.4	0.40	no
	3.6	60.5	42.7	1.78	1824.0	15.7	0.86	158	0.091	0.159	7.6	0.18	yes
	17.8	332.4	182.3	2.50	1392.5	31.4	2.25	172	0.028	0.159	7.6	0.18	no
	7.0	134.1	75.1	0.99	1892.7	44.1	2.33	205	0.083	0.401	7.6	0.38	yes
	3.2	51.5	51.5	5.00	1000.3	5.9	0.59	161	0.105	0.239	7.6	0.38	no
	9.6	183.8	100.8	1.14	5285.8	82.4	1.56	239	0.086	0.690	7.6	0.67	yes
	8.6	173.4	96.4	0.75	4736.6	184.3	3.89	209	0.072	0.693	7.6	0.67	yes
Summary of training phase	4.4	81.1	44.9	0.78	1522.5	23.4	1.54	85	0.022	0.432	7.4	0.40	yes
	3.6	62.6	57.6	3.10	5179.3	24.3	0.47	185	0.128	0.263	7.4	0.40	yes
	11.0	206.2	109.2	1.30	9922.5	73.3	0.74	180	0.045	0.404	7.4	0.40	no
	9.8	175.0	87.2	0.85	4138.4	53.9	1.30	161	0.038	0.203	7.6	0.18	no
	11.6	219.4	112.6	0.71	3108.7	37.3	1.20	167	0.036	0.191	7.6	0.18	yes
	7.8	150.6	83.8	0.99	1843.7	34.3	1.86	195	0.068	0.398	7.6	0.38	yes
	15.8	311.4	166.1	0.99	4109.0	105.9	2.58	281	0.081	0.359	7.6	0.38	no
	3.4	65.7	37.2	0.50	1931.9	37.3	1.93	122	0.057	0.740	7.6	0.67	yes
	9.8	188.5	127.6	3.60	6737.2	322.6	4.79	239	0.084	0.557	7.6	0.67	yes
Summary of validation phase	4.0	73.5	41.3	0.78	2415.0	46.8	1.94	85	0.024	0.428	7.4	0.40	no
	8.8	163.2	82.8	0.77	24360.0	114.1	0.47	250	0.104	0.438	7.4	0.40	no
	12.6	233.6	134.5	2.50	980.7	18.6	1.90	172	0.036	0.167	7.6	0.18	yes
	6.0	111.7	59.8	0.71	2589.0	27.5	1.06	140	0.044	0.202	7.6	0.18	no
	2.6	41.8	41.8	5.00	1765.2	9.8	0.56	161	0.128	0.241	7.6	0.38	no
	7.0	140.1	86.2	1.50	6892.2	71.6	1.04	160	0.050	0.365	7.6	0.38	yes

CHAPTER 4

ARTIFICIAL NEURAL NETWORKS

4.1 GENERAL

In the last two decades, Artificial Intelligence (AI) has been used in several applications in civil engineering, because of their heuristic problem-solving capabilities. Artificial neural network (ANN) is one of the AI approaches that can be classified as "machine learning". It has the ability to simulate the learning capabilities of the human brain by automating the process of knowledge acquisition and data mining. The ANN is a collection of interconnected computational elements called neurons that have performance characteristics similar to the biological neurons (Fausett 1994). This brain-like structure makes ANN models superior to knowledge-based models and mathematical formulae in making predictions that involve intuitive judgment and possess high degrees of non-linearity.

Basically, interconnections among neurons are established by weights, which are applied to all values passing through one neuron to another. Changing weights improve adaptabilities and prediction capabilities of the Neural Networks. Neural Networks are arranged in three or more layers according to their connection to the outside world.

Neurons receiving data are in the input layer; neurons carrying the results are in the output layer, and other neurons are in the hidden layers. Through the learning process, input and output data of a specific engineering problem are given and aforementioned weights among neurons are updated without requiring human development of algorithms.

4.2 GENERAL REGRESSION NEURAL NETWORKS "GRNN"

The general regression neural networks (GRNN) are similar to all artificial neural networks in its analogy to the human brain. As depicted in Figure 4.1, GRNN are three layer networks; input, hidden and output layer. The hidden layer consists of two slabs: summation and pattern units. The summation unit computes the sum of the outputs from all hidden neurons and the network's final output is obtained at the output layer where a normalization function is performed. The number of neurons in the input and output layers are as same as the number of input and output respectively, and there are hidden neurons for each training pattern in the architecture. Unlike Back-propagation neural networks, GRNN require neither time learning trials nor alarming learning time stopping knowledge. GRNN perform well for continuous function approximations and models are trained by a one-pass learning algorithm (Specht 1991).

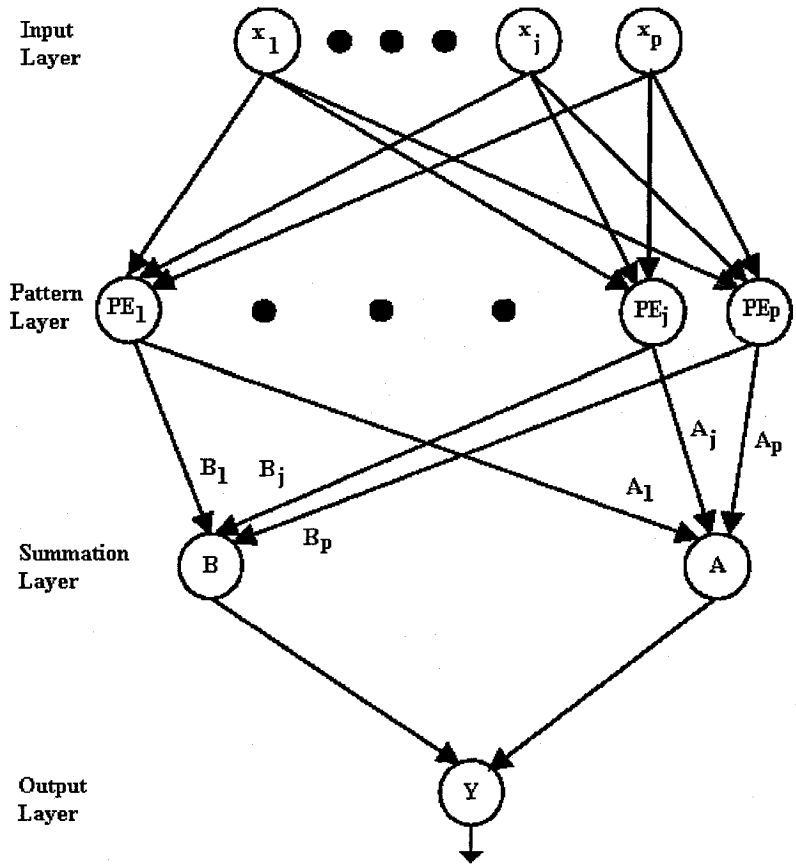

Figure 4.1: GRNN Architecture (Specht 1991)

4.3 COMPONENTS AND OPERATION OF GRNN

GRNN are selected for the development of the proposed model for the reason that they are practicable for nonlinear analysis including sparse and noisy data. GRNN, were introduced by Specht (1991) as an alternative to feed-forward neural networks and are based on nonlinear regression theory for function estimation.

In what follows below, the approach proposed by Specht (1991) is presented for clarification of the operation of GRNN. Please note that GRNN are used for decision of problem of regression. In that respect, assume y be a scalar dependant variable and system output, and **x** be a vector independent variable and system input, and let **X** be a particular measured value of **x**. Let $f(\mathbf{x}, y)$ be the joint probability density function (pdf) of **x** and y. The regression of y on **X**, by other words the conditional mean of y given **X**, is defined by the following Equation 4.1;

$$E[y \mid X] = \frac{\int_{-\infty}^{\infty} y.f(X,y)dy}{\int_{-\infty}^{\infty} f(X,y)dy} \tag{4.1}$$

If the joint pdf $f(\mathbf{X}, y)$ is known, then the expected value of regression is computed easily. However, as GRNN is a non-parametric estimator, through this approach, it is possible to compute the conditional mean of y given **X** even when the joint pdf $f(\mathbf{X}, y)$ is unknown. The joint pdf $f(\mathbf{X}, y)$ can be empirically determined from the observed data using Parzen's consistent estimators (Parzen 1962). According to Parzen window estimation, the probability estimator is given as;

$$f(X,y) = \frac{1}{(2\pi)^{p+1}\sigma^{p+1}} x \frac{1}{n}\sum_{i=1}^{n} e^{-\left(\frac{(x-x^i)^T(x-x^i)}{2\sigma^2}\right)} \cdot e^{\left(-\frac{(y-y^i)}{2\sigma^2}\right)} \tag{4.2}$$

Where,

p = Dimension of the vector variable and n is the number of sample observations.

σ = Smoothing factor

Substituting joint probability estimator in Equation 4.2 to conditional mean in Equation 4.1 yields to Equation 4.3 below;

$$\hat{y} = \frac{\sum_{i=1}^{n} e^{-\left(\frac{(x-x^i)^T(x-x^i)}{2\sigma^2}\right)} \cdot \int_{-\infty}^{\infty} y e^{\left(\frac{(y-y^i)^2}{2\sigma^2}\right)} dy}{\sum_{i=1}^{n} e^{-\left(\frac{(x-x^i)^T(x-x^i)}{2\sigma^2}\right)} \cdot \int_{-\infty}^{\infty} e^{\left(\frac{(y-y^i)^2}{2\sigma^2}\right)} dy} \tag{4.3}$$

If the scalar function is defined as $D_i^2 = (x-x^i)^T(x-x^i)$ and substituted into Equation 4.3, Equation 4.4 is evaluated as follows;

$$\hat{y} = \frac{\sum_{i=1}^{n} y_i e^{-\left(\frac{D_i^2}{2\sigma^2}\right)}}{\sum_{i=1}^{n} e^{-\left(\frac{D_i^2}{2\sigma^2}\right)}} \tag{4.4}$$

The target output corresponding to input training (w_i) can be defined in Equation 4.5 as follows;

$$w_i = e^{-\left(\frac{D_i^2}{2\sigma^2}\right)} \tag{4.5}$$

Substituting the target output in Equation 4.5 to the conditional mean in Equation 4.4 yields to Equation 4.6 (the 'heart' of GRNN) below;

$$\hat{y} = \frac{\sum_{i=1}^{n} y_i w_i}{\sum_{i=1}^{n} w_i} \tag{4.6}$$

Where;

y_i = Target output corresponding to input training vector

w_i = Output of a hidden layer neuron

In GRNN, values of w_i are assigned from the associated input training vectors. Thus, σ value is named as smoothing factor and during the GRNN training process; smoothing factors (or bandwidths) are the only weights to be calculated (Wasserman 1993). The success of the network is dependent upon the smoothing factor, but there is no intuitive method for selecting the optimal smoothing factor. If smoothing factor value is made large, distant neighbors affect the estimate at X, leading to a very smooth estimate, better generalization but poor recall. On the other hand, with a smaller value of smoothing factor wild points have too great effect on the estimate. Only a few samples plays a role, which is a good, recall but poorer generalization (Specht, 1991).

4.4 DEVELOPMENT OF GRNN MODEL

The proposed GRNN model was developed in four phases, mainly: identification phase, collection phase, implementation phase, and verification phase. An iterative procedure was followed to maximize the accuracy of the proposed model. The following subsections present a detailed explanation of the phases to the development of the GRNN model that estimates the liquefaction potential in layered soils.

4.4.1 IDENTIFICATION PHASE

In this phase, soil and seismic parameters affecting soil liquefaction potential are identified. This identification process includes assigning the input neurons the proposed GRNN model. Identification was developed in two steps according to engineering and statistical significances. Regarding engineering significance, earlier studies and model tests regarding the soil liquefaction potential evaluation were examined and the parameters involved in these studies and tests were considered. The concern in introducing various soil and seismic parameters into both SPT model and CPT model is to provide necessary information with reasonable accuracy for site characterization. Second, analysis of variance statistical test (ANOVA) table was presented to identify the importance and the significance of each of these parameters.

4.4.1.1 ENGINEERING SIGNIFICANCE OF THE VARIABLES

Soil behaves as a deformable body with increasing depth (z); hence depth is a site condition parameter and has a huge impact on soil response against its capacity to resist liquefaction. For

liquefaction to occur, ground water conditions should be sufficient to create saturated soil conditions. Thus, depth to the groundwater table (d_w) is an important consideration in identifying soils that are susceptible to liquefaction. Representing miscellaneous locations of soil layers, depth of soil specimen and ground water table, which are real world parameters than can be obtained from various globally practiced field tests, are introduced into the proposed GRNN model.

SPT blow numbers have been commonly used for characterization of liquefaction resistance and SPT procedures have been developed by researchers to obtain information for liquefaction assessment. Thus, SPT penetration resistance (N-SPT) is used as an index of liquefaction assessment model. Liquefaction potential of both cohesive and coarse-grained soils are influenced by fines content. As a compositional factor, fines content ($F \leq 75$ μm) affects both cyclic shear strength and penetration resistance. Therefore, the fines content is introduced into the model to improve the accuracy.

CPT penetration resistance has been commonly used for characterization of liquefaction resistance and CPT procedures have been developed by researchers to obtain information for liquefaction assessment. Thus, CPT test parameters, namely CPT tip resistance (q_c), CPT sleeve friction resistance (f_s), and CPT friction ratio (R_f) is used as an index of liquefaction assessment model.

It has been proven that an increase in overburden stresses increases susceptibility of soils to cyclic liquefaction. Representing geological setting of soil strata, overburden stress effects for liquefaction analysis procedures are investigated in the research of Boulanger (2003) and Seed et. al. (2003). Accordingly, total and effective overburden stresses (σ'_{vo}, σ_{vo}) are brought into the

model. Shear wave velocity (V_s) values are proven to represent the capacity of soil against liquefaction; therefore actual measured values of shear wave velocities are introduced into the network as an index of liquefaction resistance. Earthquake magnitude (M_v) and maximum horizontal acceleration at ground surface (a_{max}) characterize nature of loading, intensity of seismic ground shaking, and attenuation effects induced by the earthquakes. Obtained from strong ground networks, they are real world parameters that are crucial to introduce into the seismic model.

Conventional liquefaction potential assessment procedures heavily rely on empirical correlations such as cyclic stress ratio (τ_{av}/σ'_{vo}) for stress-based methodology and threshold acceleration (a_t/g) for strain-based methodology. Accordingly, parameters derived from field tests are used directly through empirical calculations. These correlations derived from case histories and laboratory experiments yield reliable results. Dobry et. al. (1982) showed that liquefaction resistance of saturated undrained specimens against soil liquefaction can also be quantified by threshold shear strain, which is not dependent on the method of sample preparation, and it is approximately 0.01%. By utilizing this value, acceleration corresponding to threshold shear strain value is evaluated by the strain-based assessment procedure for liquefaction occurrence. Strain-based liquefaction potential assessment procedure is idealized for sand grains and then generalized for natural soil deposits. Threshold acceleration value together with strain-based factor of safety states the exceedance of the threshold strain, which is required for liquefaction to occur. In order to evaluate the threshold acceleration, easily obtained field tests variables and earthquake characteristics are utilized. Therefore, the threshold acceleration can be considered as a real world parameter, which contributes strain-based procedure

knowledge into the complex liquefaction problem. Moreover, formulated by Seed et. al. (1971), cyclic stress ratio is a normalized measure of cyclic load severity and it represents the seismic demand on soil to liquefy. In that respect, threshold acceleration and cyclic stress ratio values are introduced into the model.

The angle at which soil resists shearing is defined as internal friction angle (ϕ'). Thus internal friction angle illustrates shearing strength. With the advent of field-testing methods, friction angle can easily consistently be estimated from SPT, CPT tests. Internal friction angle of soil is introduced into the model by using correlations based on SPT penetration blow counts in order to assess most realistic values.

4.4.1.2 STATISTICAL SIGNIFICANCE OF THE VARIABLES

The main limitation of GRNN is that it cannot ignore irrelevant inputs in the dataset. Therefore, ANOVA tables, which identify the statistical significance of the proposed input data, are crucial and required to be presented to improve the quality of the proposed data set. The ANOVA table is given in Table 4.1 for the SPT model. In the SPT model, soil specimen depth and earthquake magnitude, which are already proven to be influential parameters, were not included in the ANOVA tests.

In Table 4.1, the first column lists the parameters, which were introduced into the GRNN architectures. The next four columns respectively present following statistical characteristics: the minimum value (Min), the maximum value (Max), the mean value (μ), and the standard deviation (S). The last columns present the P-value of the ANOVA test whether for rejecting or accepting the null hypothesis (H_0). This test has a null hypothesis "Ho" that the population

means are all equal and an alternative hypothesis "Ha" that at least one population means is different. The significance level (α) criterion is used for rejecting null hypothesis. Statistically, if the P-value is less than the significance level (α) then rejects H_0, otherwise accept. If the null hypothesis is rejected then the outcome is said to be statistically significant. In significance testing, if a true null hypothesis is incorrectly rejected then Type-I error is made. By using significance level α=0.05, the probability of committing "Type-I" error is assumed to be 5%. Based on the results given in Table 4.1, it can be concluded that the listed parameters have significant effects on soil liquefaction potential as they all produced values of $P < 0.05$.

Table 4.1: SPT model ANOVA and parameter statistics

Parameter	*Min*	*Max*	μ	*S*	*P*
Correlated standard penetration blow numbers	1.06	75.18	14.48	11.37	0.034
Fines content less than 75 μm	1	100	62.99	34.28	0.000
Depth of ground water table	0.35	10	1.45	1.20	0.002
Total vertical overburden stress	12.09	408.87	144.60	98.20	0.009
Effective vertical overburden stress	7.50	233.68	82.47	52.84	0.000
Threshold acceleration	0.004	0.85	0.07	0.07	0.004
Cyclic stress ratio	0.12	0.77	0.37	0.15	0.000
Shear wave velocity	37	500	166.98	67.08	0.038
Internal friction angle	23.46	52.08	31.96	4.85	0.000
Peak horizontal acceleration at ground surface	0.18	0.67	0.38	0.15	0.000

The ANOVA table is given in Table 4.2 for the CPT model. In the CPT model, maximum horizontal acceleration at ground surface, which is already proven to be influential parameter, was not included into the ANOVA test. Based on the results given in Table 4.2, it can be concluded that the listed parameters have significant effects on soil liquefaction potential as they all produced values of $P < 0.05$.

Table 4.2: CPT model ANOVA and parameter statistics

Parameter	*Min*	*Max*	*μ*	*S*	*P*
Soil specimen depth	1.00	20.00	8.04	4.62	0.000
Total vertical overburden stress	14.1	413.3	151.19	90.92	0.000
Effective vertical overburden stress	8.5	240.9	85.69	47.72	0.000
Depth of ground water table	0.35	5.00	1.44	0.97	0.000
CPT tip resistance	9.81	32767	4667.82	6171.16	0.000
CPT sleeve friction resistance	0	890.4	50.09	55.71	0.000
CPT friction ratio	0	38.4	1.87	1.59	0.000
Shear wave velocity	37	400	167.28	63.25	0.000
Threshold acceleration	0.0018	1.3082	0.07	0.07	0.006
Cyclic stress ratio	0.115	0.752	0.36	0.16	0.014
Earthquake moment magnitude	7.40	7.60	7.51	0.10	0.001

After exploration of the engineering and statistical significance of the variables, input and output parameters for both SPT and CPT GRNN models are tabulated below:

Table 4.3: Input and output parameters of the developed SPT GRNN model

Parameter Type	*Parameter Aspect*	*Parameter Name*	*Number of Neurons*
Input	Depth	Soil specimen – Ground water	2
	Stress	Total – Effective	2
	Soil and material properties	Friction angle – Fines Content	2
	Strain	Threshold strain	1
	Liquefaction strength	Cyclic stress ratio	1
	Earthquake characteristics	Magnitude	1
	In-situ test results	SPT blow number – Shear wave velocity – max horizontal ground acceleration	3
Output	Liquefaction occurrence		1

Table 4.4: Input and output parameters of the developed CPT GRNN model

Parameter Type	*Parameter Aspect*	*Parameter Name*	*Number of Neurons*
Input	Depth	Soil specimen – Ground water	2
	Stress	Total – Effective	2
	CPT results	Tip resistance – Sleeve friction resistance – Friction ratio	3
	Strain	Threshold strain	1
	Liquefaction strength	Cyclic stress ratio	1
	Earthquake characteristics	Magnitude	1
	Other in-situ test results and measurements	Shear wave velocity – max horizontal ground acceleration	2
Output	Liquefaction occurrence		1

4.4.2 COLLECTION PHASE

Data used for training and testing the GRNN models is the main source of knowledge acquisition in this kind of models. The records obtained from the 1999 Chi-Chi, Taiwan earthquake (magnitude M_w=7.6) region and the 1999 Kocaeli, Turkey earthquake (magnitude M_w=7.4) region were used extensively in this study to develop, test, and validate the proposed GRNN models. These data, which account for 620 cases in the SPT model and 3895 cases in the CPT model, were listed in Tables 4.5 and 4.6

Table 4.5: Typical SPT Soil Data

z	$(N_1)_{60}$	$F \leq 75\mu m$	d_w	σ_{vo}	σ'_{vo}	a_t	τ_{av}/σ'_{vo}	V_s	ϕ'	M_v	a_{max}
(m)	-	*(%)*	*(m)*	*(kPa)*	*(kPa)*	*(g)*	–	*(m/s)*	*(°)*	-	*(g)*
1.0	7	87	0.64	16.1	12.5	0.13	0.32	100	30.94	7.4	0.40
2.0	12	43	0.64	34.7	21.1	0.07	0.41	100	29.80	7.4	0.40
3.0	3	57	0.64	53.9	30.3	0.10	0.43	150	24.90	7.4	0.40
4.0	5	95	0.64	72.3	38.7	0.08	0.45	150	27.54	7.4	0.40
5.0	11	91	0.64	91.6	48.0	0.06	0.45	150	30.39	7.4	0.40
6.0	12	58	0.64	111.2	57.6	0.05	0.45	150	30.95	7.4	0.40
7.0	10	93	0.64	130.2	66.6	0.05	0.45	150	30.39	7.4	0.40
8.0	9	89	0.64	147.7	74.1	0.04	0.45	150	29.80	7.4	0.40
8.8	7	100	0.64	162.2	80.6	0.04	0.45	150	29.17	7.4	0.40
9.8	34	7	0.64	183.3	91.7	0.04	0.44	160	39.90	7.4	0.40
1.1	11	89	1.65	17.7	17.7	0.12	0.25	100	26.96	7.4	0.40
4.2	10	42	5.00	67.6	67.6	0.08	0.24	161	29.17	7.6	0.38
5.8	9	25	5.00	96.8	89.0	0.08	0.26	184	29.17	7.6	0.38
9.8	15	23	1.03	198.9	112.8	0.03	0.71	149	32.49	7.6	0.67
10.8	17	18	1.03	219.8	123.9	0.03	0.70	149	33.42	7.6	0.67

Table 4.6: Typical CPT Soil Data

z	σ_{vo}	σ'_{vo}	d_w	q_c	f_s	R_f	V_s	a_t	τ_{av}/σ'_{vo}	M_v	a_{max}
(m)	*(kPa)*	*(kPa)*	*(m)*	*(kPa)*	*(kPa)*	*(-)*	*(m/s)*	*(g)*	*(-)*	*(-)*	*(g)*
1.6	29.0	20.8	0.78	577.5	11.2	1.9	105	0.09	0.35	7.4	0.4
5.2	93.7	49.3	0.77	1050.0	23.4	2.2	105	0.03	0.45	7.4	0.4
7.6	138.4	70.5	0.82	10570.0	75.9	0.7	250	0.12	0.45	7.4	0.4
5.8	107.0	56.0	0.71	787.5	10.2	1.3	85	0.02	0.45	7.4	0.4
3.6	62.6	57.6	3.10	5179.3	24.3	0.5	185	0.13	0.26	7.4	0.4
3.8	66.6	59.6	3.10	7504.7	31.1	0.4	185	0.12	0.27	7.4	0.4
9.8	198.2	117.0	1.68	28169.0	103.0	0.4	400	0.24	0.37	7.4	0.4
4.0	68.5	43.5	1.50	3360.0	37.7	1.1	85	0.02	0.38	7.4	0.4
4.4	77.0	37.4	0.44	945.0	26.5	2.8	85	0.02	0.49	7.4	0.4
7.2	134.9	76.2	1.34	845.6	9.7	1.1	180	0.06	0.40	7.4	0.4
7.4	138.8	78.1	1.34	3963.8	51.6	1.3	180	0.06	0.40	7.4	0.4
9.0	165.6	88.6	1.30	1470.0	31.6	2.1	180	0.05	0.41	7.4	0.4
2.0	36.1	33.0	1.69	1268.4	7.8	0.6	145	0.14	0.27	7.4	0.4
11.6	224.4	125.3	1.69	1744.1	74.9	4.3	170	0.04	0.38	7.4	0.4
7.8	146.3	73.3	0.50	23677.0	59.1	0.2	299	0.17	0.45	7.4	0.4
6.6	121.3	71.6	1.64	5722.5	43.8	0.8	49	0.01	0.39	7.4	0.4

4.4.2.1 1999 KOCAELI, TURKEY EARTHQUAKE

A collaborative research program was carried out by University of California- Berkeley, Brigham Young University, University of California-Los Angeles, ZETAS corporation, Sakarya University, Bogazici University and Middle East Technical University with the support of the U.S National Science Foundation, California Department of Transportation, California Energy Commission, and Pacific Gas and Electric Company in the region following the 1999 Kocaeli, Turkey earthquake. A total of 135 CPT profiles (of which 19 were seismic CPTs) and 46 soil borings with multiple SPT (often at 0.8 m spacing) were completed in the city of Adapazari. Details of this site investigation program are available at http://peer.berkeley.edu/turkey/adapazari/

4.4.2.2 1999 CHI-CHI, TAIWAN EARTHQUAKE

A series of site investigation programs were undertaken in 2000 by researchers with the National Center for Research in Earthquake (NCREE) in Taiwan and in 2001-2002 by the authors with funding from Pacific Earthquake Engineering Research Center (PEER). The PEER and NCREE site investigation programs resulted in a total of 92 cone penetration test (CPT) soundings (of which 63 were seismic CPTs) and 98 soil borings with standard penetration testing (SPT) (typically at 1.0 m spacing). The majority of the NCREE work was performed in the city of Yuanlin, whereas the entirety of the PEER work and some of the NCREE work was performed in the cities of Nantou and Wufeng. Results of both site investigation programs are synthesized at the address http://peer.berkeley.edu/lifelines/research_projects/3A02/.

4.4.3 IMPLEMENTATION PHASE

For the implementation of the proposed models, the Neural Network software (NeuroShell 2) developed by the Ward Systems Group, in United States was used for training, testing and validating the GRNN model. This software is capable of implementing different Neural Network architectures including BPNN, GRNN, and PNN. The following are the basic steps carried out for model implementation.

4.4.3.1 Binary-Value Transformation

The symbolic output parameter, which is the liquefaction decision, is transformed into a numeric parameter due to the fact that neural networks deal only with numbers (Nelson and Illingworth 1991). In that respect, the liquefaction potential is characterized by 1 output neuron; where the binary number 1 represents the occurrence of liquefaction and 0 represents the nonoccurrence of liquefaction.

4.4.3.2 Data Division

Moreover, as given in Table 4.7 below, SPT & CPT databases were randomly categorized into three subsets namely training, testing, and validation sets. Training sets generate the algorithm with best smoothing parameter. Testing sets are used for observing the capabilities of the generated algorithm to assess intricate relationships amid input and output values. Validation sets are used for applying the trained algorithm to separate dataset, which was not introduced to the network before. Therefore, validation set can be regarded as the real test for the

performance of the model. Neural Networks perform well as long as large volumes of data covering to all possible governing parameters and field conditions.

Table 4.7: Distribution of data for GRNN Modeling

Database	***SPT Database***			***CPT Database***		
Earthquake	***Turkey***	***Taiwan***	***Total***	***Turkey***	***Taiwan***	***Total***
Training	35%	31%	67%	35%	40%	75%
Testing	10%	9%	18%	6%	7%	13%
Forecast	8%	7%	15%	5%	6%	12%
Total	53%	47%	100%	47%	53%	100%

4.4.3.3 GRNN Architecture Design

Configuring the network architecture is one of the most crucial stages in model development. As schematically shown in Figure 4.2 below; GRNN is a three layer network where the number of neurons in the input layer (Slab 1) is the number of inputs in your problem, the number of neurons in the output layer (Slab 3) corresponds to the number of outputs, and there must be one neuron for each training pattern in the hidden layer (Slab 2), however, it is possible to increase the number of the neurons in the hidden if adding more pattern data is projected.

Input values are required to be scaled to a numeric range so that the network deals with them efficiently. Roughly, there are two types of scaling, namely linear and non-linear scaling. In this study, linear scaling [0,1] is utilized. In other words, data from 0 to 100 is scaled to [0,1].

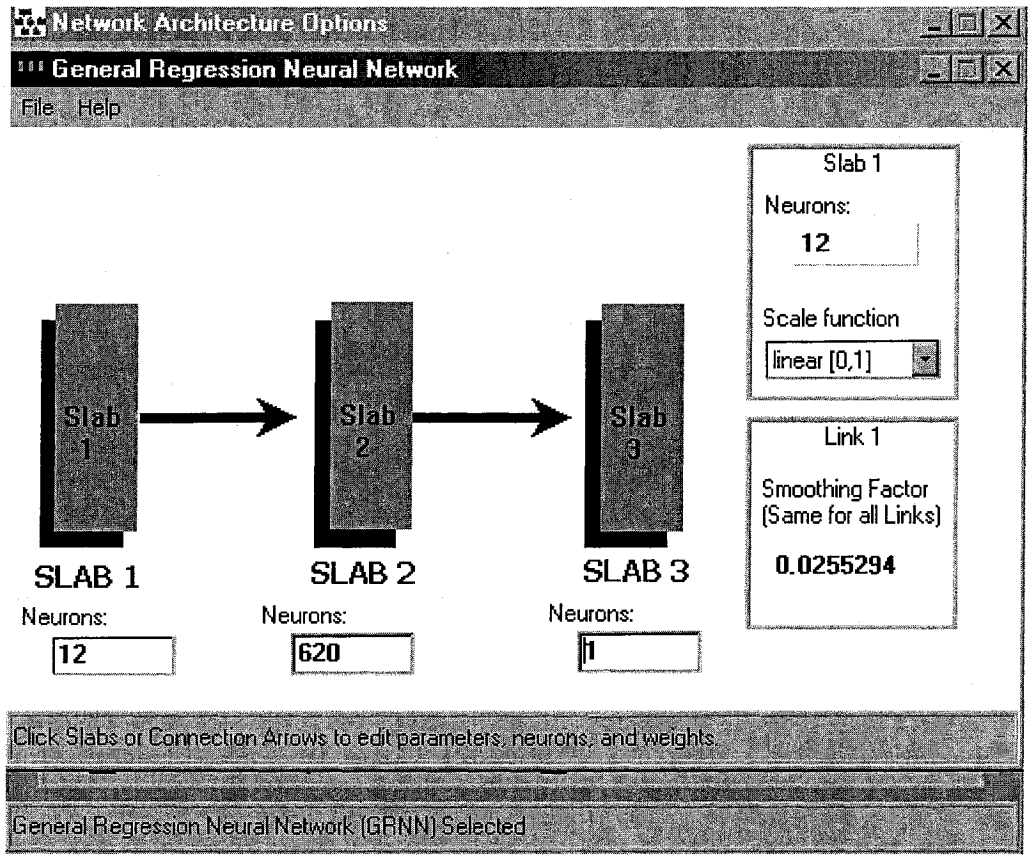

Figure 4.2: GRNN architecture design module

4.4.3.4 Training Criteria

In GRNN, the distance of the sample pattern from the given training set is measured. The training data is represented in N dimensional space, where N is the number of inputs introduced into the network. In this study, 'city block distance' is measured. As shown in Equation 4.7 below, the City Block distance metric is the sum of the absolute values of the differences in all dimensions between the pattern and the weight vector for that neuron (Neuroshell 2, 1996)

$$\hat{y} = \frac{\sum_{i=1}^{n} y^i \exp(-\frac{C_i}{\sigma})}{\sum_{i=1}^{n} \exp(-\frac{C_i}{\sigma})} \tag{4.7}$$

Where

$$C_i = \sum_{j=1}^{p} \left| X_j - X_j^i \right| \tag{4.8}$$

4.4.3.5 GRNN Learning

In this phase, GRNN training data are presented into the network. Network's outcome in the training data is applied to the testing data and the best smoothing factor for the network was explored. The value of the smoothing factor giving the smallest error is used in the final network. The objective is minimizing the mean squared error of the test set: therefore, amid presented test data, random testing datasets are generated in order to observe the network's performance. Given in Figures 4.3 and 4.4, the mean squared error for the test set is compared to the number of generations for both SPT and CPT Model.

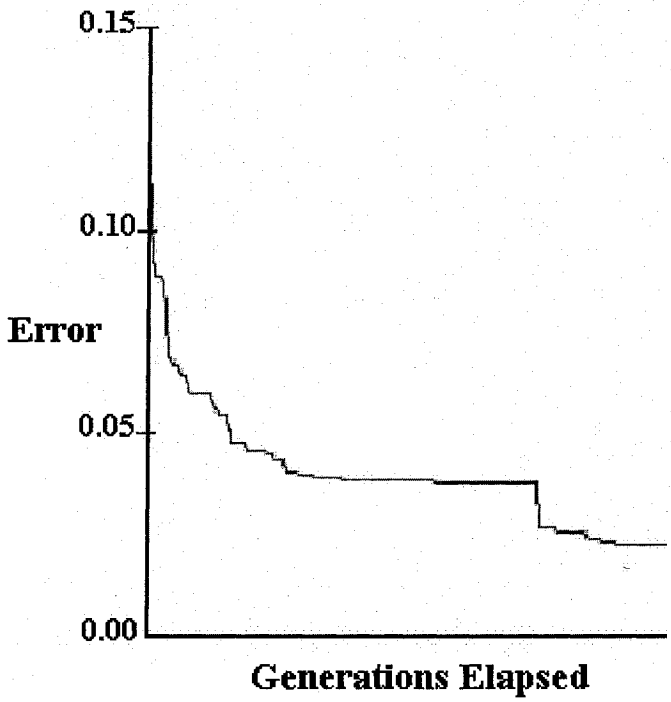

Figure 4.3 SPT model training graphic

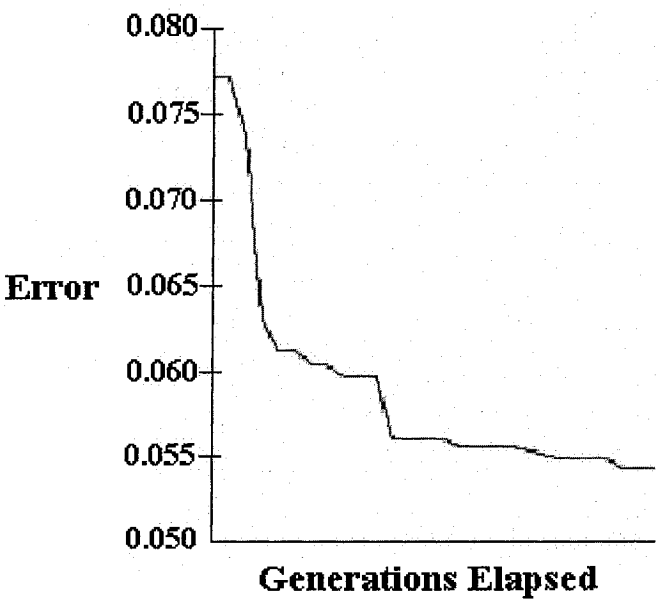

Figure 4.4: CPT model training graphic

While applying the network's outcome to the test patterns, statistical values, given in Table 4.8 below, are utilized to understand network's performance as learning progresses. In column 2 and 3, total number of training and testing patterns are shown respectively. Column 3 displays the number of times the test set has been propagated through the network with different smoothing factor adjustments. Column 4 shows the value of the smoothing factor giving the smallest error. Column 5 shows the value of the mean squared error calculated by the best smoothing factor. Please note that those minimum mean squared errors are internal to the net and limited to the test patterns.

Table 4.8: GRNN learning statistics

Network training statistics	***SPT Model***	***CPT Model***
Number of training patterns	413	2922
Number of test patterns	112	521
Smoothing test individuals	4540	559
Current best smoothing factor	0.0255	0.0332
Minimum mean squared error*	0.0218	0.0542

*Please see Figures 4.3 and 4.4

As the last step of implementation, trained neural network is applied to data file to produce predictions for each data pairs introduced into the model. In that step, the coefficient of multiple determination value (R) is evaluated by the Equation 4.9 below:

$$R^2 = 1 - \frac{\sum (y - \hat{y})^2}{\sum (y - \bar{y})^2} \tag{4.9}$$

Where;

y = Actual value

$\hat{y}$ = Predicted value of y

$\bar{y}$ = Mean value of y

R-squared value compares the accuracy of the model results to the actual values. A perfect fit results in a R-squared value of 1, and a poor fit results in 0.

4.4.3.6 SPT MODEL IMPLEMENTATION PHASE

In the proposed GRNN model based on SPT database, smoothing factor of σ=0.02552 was used for soil liquefaction potential estimation. In this proposed GRNN model, the coefficient of multiple determination value (R^2) is 96.4% for the training phase and 83.6% for the validation phase. The error limit for the analysis was taken as $\pm$ 30%. This means that when the difference between the target output and the network result within this range, the result is considered to be incorrect. Error distribution through patterns is given in Figure 4.5.

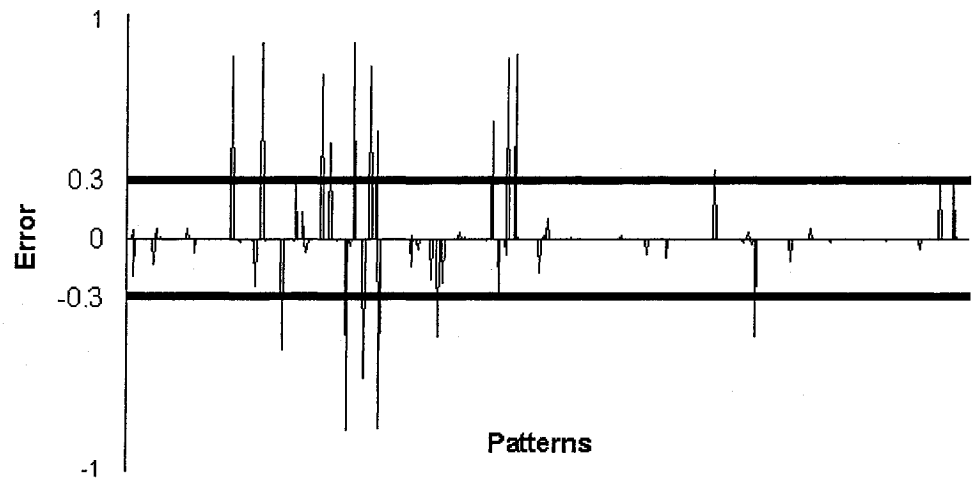

Figure 4.5: Error through Patterns

Figure 4.6 presents the results of the sensitivity study for the parameters impacting liquefaction potential in the SPT model.

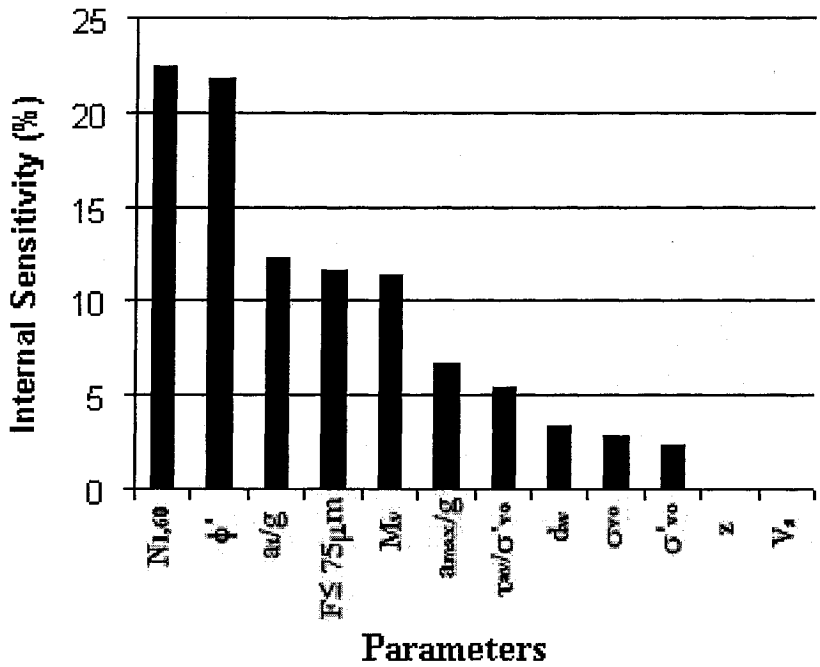

Figure 4.6: Parameter Sensitivity Study of the SPT model

4.4.3.7 CPT MODEL IMPLEMENTATION PHASE

In the CPT model, GRNN approach used for soil liquefaction potential estimations with a smoothing factor of σ=0.0332. In this proposed GRNN model, the coefficient of multiple determination value (R^2) is 94.4% for the training phase and 83.3% for the validation phase. The error limit for the analysis is taken as 0.3 (i.e., 30%). This means that with the difference between the target output and network result is greater than 0.30, the result is considered to be incorrect. Error distribution through patterns is depicted in Figure 4.7.

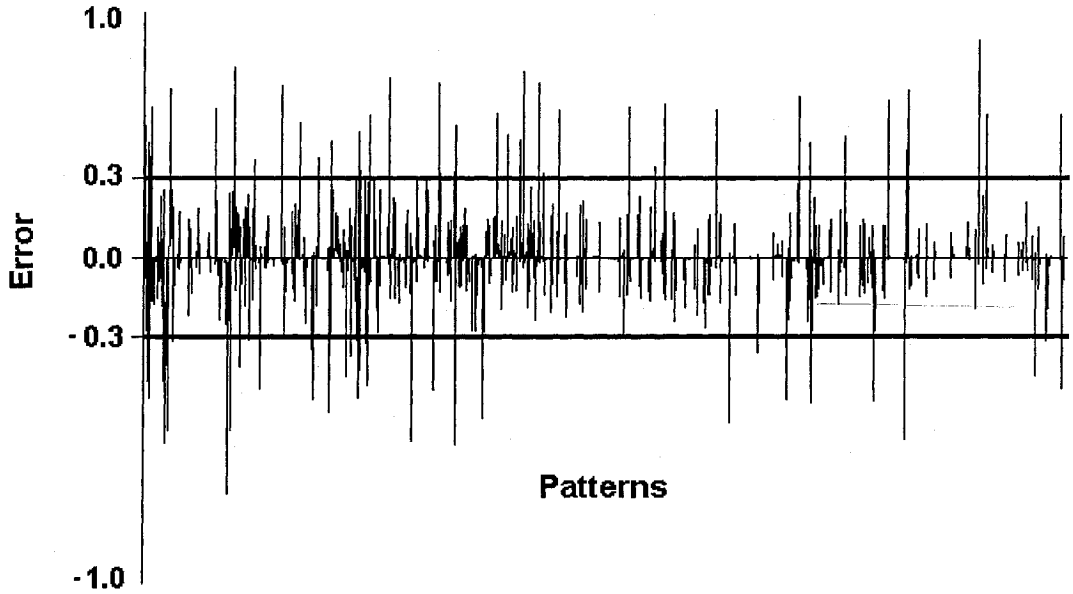

Figure 4.7: Error through patterns

In the parameter sensitivity study of the CPT model, most influential parameters impacting liquefaction assessment are outlined and given in Figure 4.8.

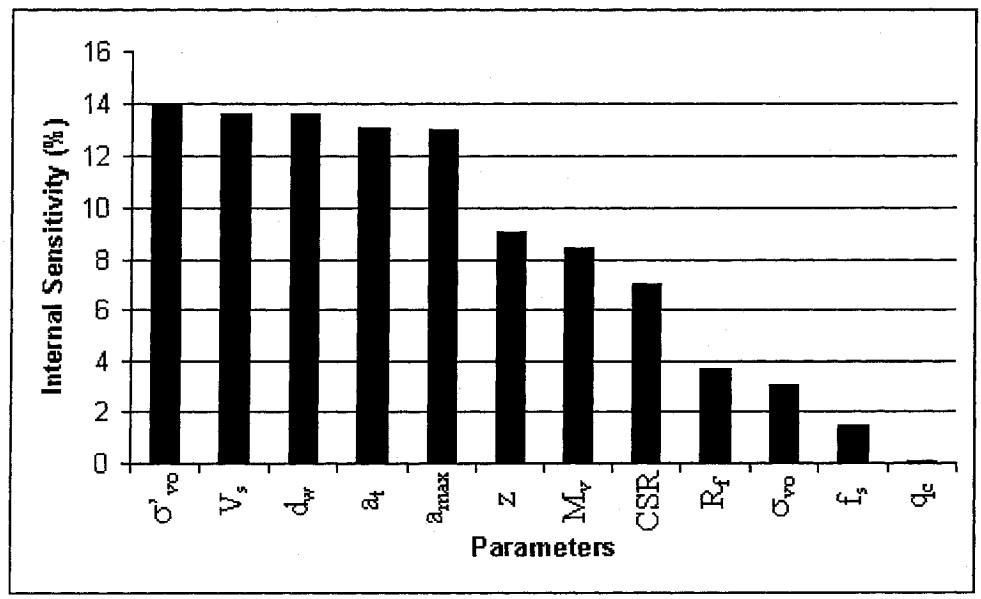

Figure 4.8: Parameter Sensitivity Study

The liquefaction potential is characterized by 1 output neuron; where the binary number 1 represents the occurrence of liquefaction and 0 represents the non-occurrence of liquefaction.

4.4 VALIDATION PHASE

In this phase, model accuracy and efficiency were examined by making prediction against case records, which were not used during model training and testing. In this phase, the proposed algorithm does not require human development of the proposed model: it rather confirms the architecture's prediction capabilities of the model.

4.4.1 SPT MODEL VALIDATION PHASE

In the SPT model, validation data approximately corresponds to 15% of the dataset selected from Kocaeli, Turkey and Chi-Chi, Taiwan earthquakes case histories. The results of this phase are also given in Table 3.11 and summarized in Table 4.9.

Table 4.9: Results of the SPT based GRNN model

	Overall			*Taiwan Earthquake*			*Turkey Earthquake*		
	Case Records	***Error***	***Success***	***Case Records***	***Error***	***Success***	***Case records***	***Error***	***Success***
Train	413	0	100%	193	0	100%	220	0	100%
Test	112	8	92.9%	53	3	94.3%	59	5	92%
Forecast	95	5	94.7%	44	0	100%	51	5	90%
Total	620	13	97.9%	290	3	99.0%	330	10	97%

Network's outcome in favor of soil liquefaction occurrence/nonoccurrence for both earthquake cases is given in Figure 4.9.

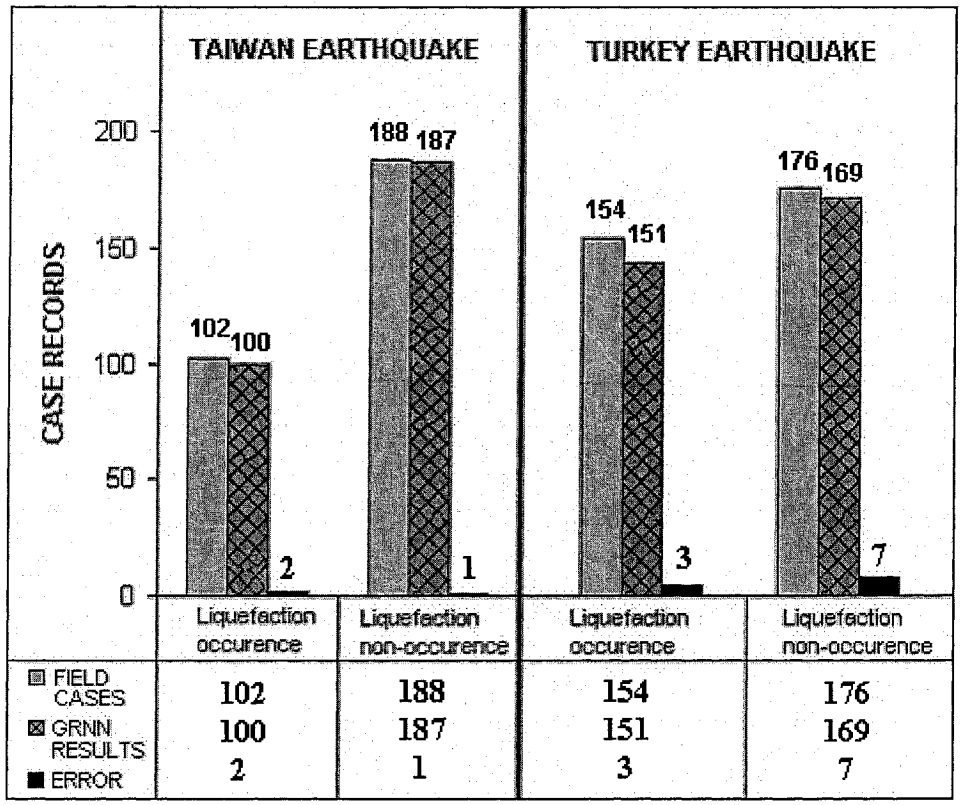

Figure 4.9: SPT model's performance on soil liquefaction potential

4.4.2 CPT MODEL VALIDATION PHASE

In the CPT model, validation data, approximately corresponds to 12% of the dataset, it was randomly selected from Kocaeli, Turkey and Chi-Chi, Taiwan earthquakes case histories. The results of this phase are also given in the Table 3.12, and summarized in Table 4.10.

Table 4.10: Results of the CPT based GRNN Model

	Overall			*Taiwan Earthquake*			*Turkey Earthquake*		
	Case Records	*Error*	*Success*	*Case Records*	*Error*	*Success*	*Case records*	*Error*	*Success*
Train	2922	10	99.66%	1562	0	100.00%	1360	10	99.26%
Test	521	46	91.17%	282	15	94.68%	239	31	87.03%
Forecast	452	27	94.03%	239	8	96.65%	213	19	91.08%
Total	3895	83	97.87%	2083	23	98.90%	1812	60	96.69%

Network's outcome in favor of soil liquefaction occurrence/nonoccurrence for both earthquake cases is given in Figure 4.10 below.

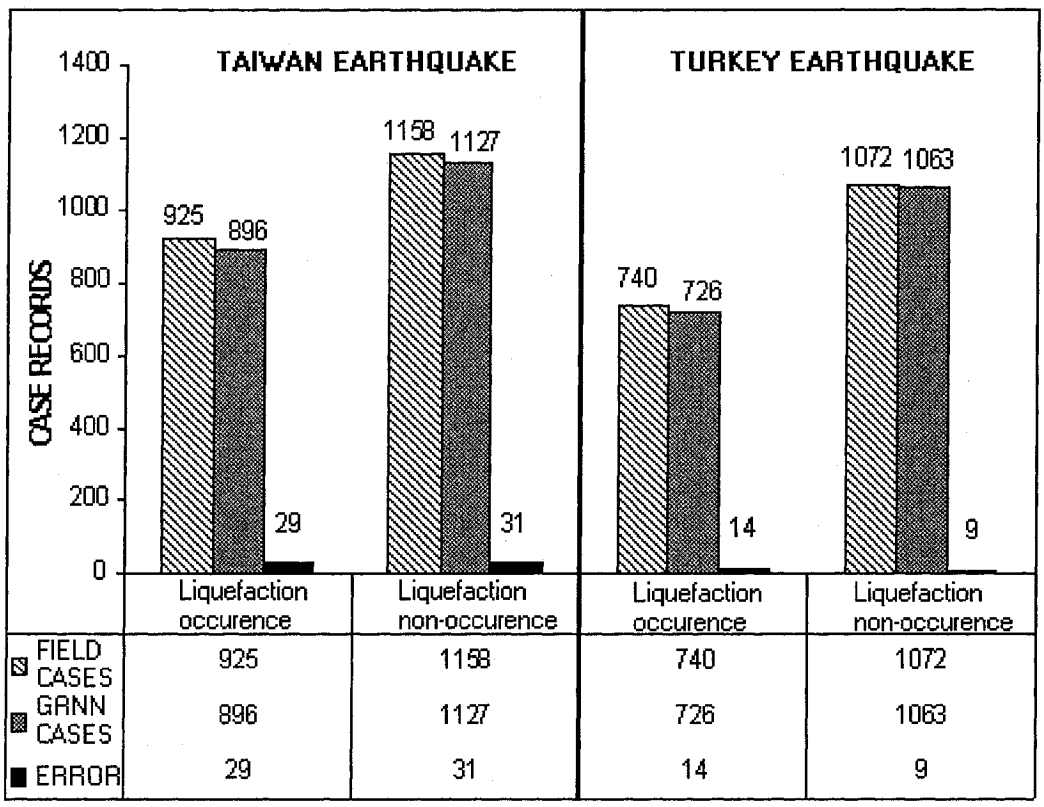

Figure 4.10: CPT model's performance on soil liquefaction potential

CHAPTER 5

CONCLUSION AND RECOMMENDATIONS

5.1 SUMMARY

As we are racing into the 21st century, population density of some communities is getting larger on daily basis. Furthermore, the damages caused by earthquakes are extensive and costly. Soil liquefaction potential, is considered one of features of earthquakes, which is regarded as complex geotechnical engineering problem that is not well understood yet; due to its mysterious internal mechanism. Therefore, researchers had focused on conducting experimental and field tests and developing design theories to predict soil liquefaction potential in soil deposits. This research was directed to predict soil liquefaction using the governing soil and seismic parameters.

The literature review revealed that prediction of occurrence and non-occurrence of soil liquefaction has been investigated through numerous empirical methods. These empirical methods were based on field data, which have been developed according to the observations in the previous earthquakes. Furthermore, in-situ based empirical methods are regarded as cost efficient for geotechnical engineers throughout much of the world to employ them.

The proposed model explores the feasibility of addressing soil and seismic parameters acquired from the two most widely used in field testing, namely standard penetration test and cone penetration test. Therefore, the measurements of these tests are incorporated into one model.

A computational knowledge based approach, known as General Regression Neural Network (GRNN), is presented to predict the soil liquefaction potential in layered soils.

Collected from Turkey and Taiwan earthquake regions following the devastating earthquakes took place in 1999, extensive in-situ and laboratory tests were performed. In the present study, a total of 70 CPT profiles and 63 SPT borings have been used to generate a total of 620 case records for the SPT database and 3895 case records for the CPT database. These data were used for training and validating of the proposed GRNN model.

In order to identify the input parameters of the proposed networks, the analysis of variance (ANOVA) statistical measures were carried out for both SPT & CPT model database. Additionally, sensitivity analysis was conducted to determine the parameters, which govern this behavior. Twelve soil and seismic parameters for SPT model and twelve soil and seismic parameters for CPT model, which characterizing the soil type and material properties, seismic attenuation characteristics, magnitude and nature of loads, and other site conditions including stress, strain, strength, saturation and seismological aspects were selected and incorporated into the network.

The results produced by the proposed "GRNN" models compared well with the available field results. It provides a viable liquefaction potential assessment tool that assist geotechnical engineers in making an accurate and realistic predictions. Furthermore, this study integrates knowledge learned from the two devastating earthquakes to the ongoing development of soil liquefaction analysis.

5.2 CONCLUSIONS

Based on the results of this investigation, it can be reported that Neural Networks are powerful computational tool to analyze the complex relationship between soil and seismic parameters for liquefaction potential analysis in layered soils. The proposed GRNN model is a quick and reliable tool for estimating the liquefaction potential without performing any manual work. In addition, the proposed model can be easily updated to incorporate new data and to accommodate new parameters. Based on the output of this research, the following conclusions can be made:

1. CPT model develops a Neural Network architecture, which examines soil liquefaction potential in CPT based soil data, where liquefaction decision, in the form occurrence/non-occurrence, is imported from SPT test results. In this respect, verification of the viability of SPT-to-CPT data conversion, which is the main limitation of simplified techniques, is tested.

2. Based on the sensitivity analysis of SPT parameters, it was noted that SPT penetration resistance is the most influential parameter, and the shear wave velocity is the least significant parameter. Results are highly consistent with information reported in the literature, as reported by Seed et. al. 2003, namely that the shear wave velocity is a very small-strain measurement and correlates poorly with a much larger strain problem such as liquefaction (Seed et. al. 2003). Furthermore, the sensitivity analysis of CPT parameters revealed that the most effective parameter for CPT model is the effective overburden stress of soil.

3. It is of interest to note that assessments, which were developed based on applying only one type of the existing seismic assessment and liquefaction potential procedures, have failed to make well predictions following the Turkey and Taiwan earthquakes (Stewart et. al. 2001; Peer, 2003). However, the proposed comprehensive Neural Network model consists of all independent soil and seismic parameters proven to be influential for decision making; therefore, eliminates the shortcomings of the existing design formulae.

4. New soil and seismic parameters, which were ignored in previous works, are incorporated in the present model. With increasing the number of input parameters, it was noted that distinct improvements in the performance of the Neural Network models were observed.

5. When compared to the previous works, this proposed GRNN model has a much larger data set in terms of size and quality, which globally cover all possible variation of the problem stated. Therefore, with a larger number of data, a more accurate sensitivity analysis is attained for soil and seismic parameters.

6. Furthermore, this study integrates knowledge learned from the two devastating earthquakes on the ongoing development of soil liquefaction analysis.

5.3 RECOMMENDATIONS FOR FUTURE RESEARCH

When future field case records became available, the performance of the Neural Network will be significantly enhanced. In addition to the network configuration and architecture tried in this research, different network architectures can be used in the training of the network by changing the network's internal parameters. Different models can also be constructed by changing the input parameters, and network performance for these models should be investigated. Besides, GRNN algorithm used in this study, other well-known Neural Network types such as probabilistic neural network, PNN and polynomial neural network, GMDH whose learning algorithms are different can also be used.

REFERENCES

Abu Keifa, M. A. (1998). "General regression neural networks for driven piles in cohesionless soils." *Journal of Geotechnical and Geoenvironmental Engineering Division,* ASCE, 124(12), 1177-1185

Ambraseys, N. N. (1988) "Engineering seismology" Earthquake Engrg. And Struct. Dynamics, 17, 1-105

Andrus R.D. and Stokoe K.H. (1997) Liquefaction resistance based on shear wave velocity, Proceedings of the NCEER Workshop on Evaluation of Liquefaction Resistance in Soils. Technical Report NCEER-97-0022, National Center for Earthquake Engineering Research, State University of New York at Buffalo, Buffalo, N.Y, 89-128.

Arango, I. (1996). "Magnitude scaling factors for soil liquefaction evaluations." J. Geotech. Engrg., ASCE, 122(11), 929-936

Bakir, B.S., Sucuoglu, H. and Yilmaz, T. (2002) "An Overview of Local Site Effects and the Associated Building Damage in Adapazari during the 17 August 1999 Izmit Earthquake", Bull. Seismological Society of America, Vol. 92, No. 1, pp. 509-526.

Barai S and Agarwal G. Studies on Instance Based Learning Models for Liquefaction Potential Assessment, Electronic Journal of Geotechnical Engineering (http://www.ejge.com/2002/Ppr0235/Ppr0235.htm), 2002

Berrill, J.B. and Davis, R.O. (1985). "Energy dissipation and seismic liquefaction of sands: revised model." *Soils and Foundations*, 25(2), 106-118.

Boulanger, R. W. (2003)."High overburden stress effects in liquefaction analyses." Journal of Geotechnical and Geoenvironmental Engineering, ASCE, 129(12), 1071-1082

Castro, G. (1995). ''Empirical methods in liquefaction evaluation.'' Primer Ciclo d Conferencias Internationales, Leonardo Zeevaert, Universidad Nacional Autonoma de Mexico, Mexico City.

Christian, J.T. and Swiger, W.F., (1995) "Statistics of liquefaction and SPT results" Journal of the Geotechnical Engineering Division, ASCE, Vol. 101, no. GT11, pp. 1135-1150

Das, B. M. (1999) "Principles of foundation engineering." Brooks / Cole Publishing Company, California, USA

DeAlba, P., Seed, H.B., and Chan, C.K., (1976) "Sand liquefaction in large scale simple shear tests" Journal of Geotechnical Engineering Division, ASCE, Vol. 102, no. GT9, pp. 909-927.

Dobry R., Stokoe K.H, Ladd R.S. and Yound T.L. (1981) "Liquefaction susceptibility from S wave velocity" ASCE National Convention, St. Louis, Missouri, USA, October 26-31, preprint 81-544.

Dobry R., Ladd R.S., Yokel F.Y., Chung R.M. and Powell, D. (1982) "Prediction of pore water pressure buildup and liquefaction of sands during earthquakes by the cyclic strain method: NBS Building Science Series 138" U.S. Dept. of Commerce, 152 p.

Dunhum, J.W.,(1954). "Pile Foundations for Buildings.", Proc., ASCE, *J. Soil Mech. Found. Div.,*80 (SM9), Proc. Paper 385, 1-21.

Fausett, L., (1994) "Fundamentals of Neural Networks: architectures, and applications.", Prentice Hall, Upper Saddle River, NJ, USA.

Finn W.D.L., Ledbetter R.H., and Wu G. (1994) "Liquefaction in silty soils: Design and analysis, Ground Failures under Seismic Conditions, Geotechnical Special Publication 44, ASCE, New York, 51-76.

Flood I. and Kartam N. (1994) "Neural networks in civil engineering. I: Principles and understanding" J. Computing Civ. Engrg., ASCE, 8, No.2, 131-148.

Ghaboussi J. (1992) « Potential applications of neuro-biological computational models in geotechnical engineering. Numerical models in geotechnics" G.N. Pande and S. Pietruszezak, eds., Balkema, Rotterdam, The Netherlands, 543-555

Gilstrap S.D, and Youd, T.L. CPT based liquefaction resistance analyses evaluated using case histories. Technical Report CEG-98-01,Department of Civil and Environmental Engineering, Brigham Young University, Prove, Utah, 1998

Goh, A.T.C., (1995) "Seismic liquefaction potential assessed by Neural Networks. Journal of Geotechnical and Geoenvironmental Engineering Division, ASCE, 120 (9), 1467-1480.

Goh, A.T.C. (1995). "Empirical design in geotechnics using Neural Networks." *Geotechnique*, 45(4), 709-714.

Goh A.T.C., (1996) "Neural Network modeling of CPT seismic liquefaction data, Journal of Geotechnical and Geoenvironmental Engineering Division, 122, No.1, 70-73.

Goh A.T.C., (2002) "Probabilistic neural network for evaluating seismic liquefaction potential" *Canadian Geotechnical Journal*, 39, 219–232.

Hanna, A.M., Morcous, G. and Helmy, M. (2004). "Efficiency of pile groups driven in cohesionless soil using artificial neural networks." *Canadian Geotechnical Journal*, In-press.

Hammerstrom D. (1993) "Working with neural networks" *IEEE Spectrum*, 46-53, Processing, 4, No.2, 4-22.

Hardin B.O. and Drnevich V.P. (1972) "Shear modulus and damping in soil: measurement and parameter effects" Journal of the Soil Mechanics and Foundations Division, ASCE, 98, 603-624.

Ishihara, K. (1985) "Stability of natural deposits during earthquakes" Proceedings, 11th International Conference on Soil Mechanics and Foundation Engineering, Vol. 1, pp. 321-376

Ishihara, K. (1993). "Liquefaction and flow failure during earthquakes." *Géotechnique*, 43(3), 351-415.

Juang C.H., Chen C.J. and Tien Y.-M., (1999) "Appraising cone penetration test based liquefaction resistance evaluation methods: artificial neural network approach" Canadian Geotechnical Journal, 36, 443–454

Juang, C.H., Chen, C.J., Jiang, T. and Andrus, R.D. (2000). "Risk-based liquefaction potential evaluation using standard penetration tests." *Canadian Geotechnical Journal*, 37, 1195-1208.

Kayen, R. E., Mitchell, J. K., Seed, R. B., Lodge, A., Nishio, S., and Coutinho, R. (1992). ''Evaluation of SPT-, CPT-, and shear wave-based methods for liquefaction potential assessment using Loma Prieta data.'' *Proc., 4th Japan-U.S. Workshop on Earthquake-Resistant Des. of Lifeline Fac. and Countermeasures for Soil Liquefaction*, Vol. 1, 177–204.

Kim, B. T., and Kim, Y. S. (2002). "Lateral load-deflection modeling of group pile using artificial neural networks." *Proceedings of the International Deep Foundation Congress*, Orlando, FL.

Kolb B.H & Shockly R. (1957). " Typical Properties of Soils from Selected Environments of Deposition within the Mississippi Alluvial Valley." *J. Soil Mech. Found. Div*, 83(3), 1-14.

Lai, S.Y., Hsu, S.C., and Hsieh M.J. (2004). "Discriminant model for evaluating soil liquefaction potential using cone penetration test data" Journal of the Geotechnical Engineering Division, ASCE, 130 (12), 1271-1282.

Nelson, M. M. and Illingworth, W. T. (1991), A practical guide to Neural Nets, Addison – Wesley, New York

Liao, S., and Whitman, R. V. (1986a). "Overburden correction factors for SPT in sand." *J. Geotech. Engrg.*, ASCE, 112(3), 373–377.

Liao, S. S. C., and Whitman, R. V. (1986b). "Catalogue of liquefaction and non-liquefaction occurrences during earthquakes." *Res. Rep.*, Dept. of Civ. Engrg., Massachusetts Institute of Technology, Cambridge, Mass.

Liao, S. S. C., Veneziano, D., and Whitman, R. V. (1988). "Regression models for evaluating liquefaction probability." *J. Geotech. Engrg.*, ASCE, 114(4), 389–411.

NCEER (1997). "Proceedings of the NCEER workshop on evaluation of liquefaction resistance of soils" Edited by Youd, T.L., Idriss, I. M., Technical Report No. NCEER-97-0022, December 31, 1997

NeuroSHELL 2 user's manual – version 3.0 (1996) Frederick M.D., Ward Systems Group, Inc., USA

Olsen, R.S. (1997). "Cyclic liquefaction based on the cone penetrometer test" *Proc., NCEER Workshop on Evaluation of Liquefaction Resistance of Soil,* T.L. Youd and I.M. Idriss, eds., NCEER-97-0022.

Parzen, E. (1962). "On estimation of a probability density function and mode." *Annals. Of Mathematical Statistics*, 33, 1065-1076

PEER, Pacific Earthquake Engineering Research, 2003, http://peer.berkeley.edu

Pyke, R. (2003) "Discussion of Liquefaction resistance of soils: Summary report from the 1996 NCEER and 1998 NCEER/NSF Workshops on evaluation of liquefaction resistance of soils by Youd T.L., Idriss I.M., Andrus R.D., Arango I., Castro G., Christian J.T., Dobry R., Finn W.D., Harder L.F., Hynes M.E., Ishiara K., Koester J.P., liao S.S.C., Marcuson W.F., Martin G.R., Mitchell J.K., Moriwaki Y., Power M.S., Robertson P.K., Seed R.B., and Stokoe K.H., II" ASCE,, J. Geotech. Engrg., ASCE, 127(10), 817-833

Rauch, A.F. (1997). "EPOLLS: An Empirical Method for Prediciting Surface Displacements Due to Liquefaction-Induced Lateral Spreading in Earthquakes", PhD Dissertation, Virginia Polytechnic Institute and State University

Risk Management Solutions Inc. (2000) "Event Report: Chi-Chi, Taiwan Earthquake" CA, USA

Robertson P.K and C.E. Wride. Evaluating Cyclic Liquefaction Potential Using the Cone Penetration Test, Canadian Geotech. J., 1998, Ottawa, Vol. 35, No. 3, pp. 442-459.

Scawthorn, C. 2000. Earthquakes of 1999. *Euro Conf. On Global Change and Catastrophe Risk Management: Earthquake Risks in Europe*, Laxenburg Austria

Seed S.B. and Idriss I.M. (1971) Simplified procedure for evaluating soil liquefaction potential. *J. Soil Mech. Found. Div.*, 97, No.9, 1249-1273.

Seed, H. B. (1979). ''Soil liquefaction and cyclic mobility evaluation for level ground during earthquakes.'' *J. Geotech. Engrg. Div.*, ASCE, 105(2), 201–255.

Seed H.B., Tokimatsu K., Harder L.F. and Chung, R. (1985) Influence of SPT procedures in soil liquefaction resistance evaluations. *Journal of Geotechnical Engineering, ASCE,* 111, No.12, 861-878.

Seed R.B. and Harder L.F. (1990) "SPT-based analysis of cyclic pore pressure generation and undrained residual strength" In J.M. Duncan, editor, Proc. H. Bolton Seed Memorial Symp, volume 2, pp. 351-376.

Seed H.B. and Idriss I.M. (1982) "Ground motions and soil liquefaction during earthquake, Monograph Series" Earthquake Engineering Research Institute, Berkeley, Calif.

Seed H.B. and Idriss I.M. and Arango I. (1983) "Evaluation of Liquefaction Potential using Field Performance Data" Journal of Geotechnical Engg, ASCE, 109, Vol.3, 458-482.

Seed, H.B., Mori, K., and Chan C.K., (1977) "Influence of seismic history in liquefaction of sands" Journal of the Geotechnical Engineering Division, ASCE, Vol 103, no GT4, pp. 246-270

Seed, R.B., Cetin, K.O., Moss, R.E.S., Kammerer A.M., Wu, J., Pestana, J.M., Riemer, M.F., Sancio, R.B., Bray, J.D., Kayen, R.E., Faris, A. (2003) "Recent advances in soil liquefaction engineering: A unified and consistent framework" 26th Annual ASCE Los Angeles Geotechnical Spring Seminar, Long Beach, California.

Shanin, M.A., Maier, H.R. and Jaska, M.B. (2002). "Predicting settlement of shallow foundations using neural networks." *Journal of Geotechnical and Geoenvironmental Engineering Division,* ASCE, 128(9), 785-793.

Specht D.F., (1990) "Probabilistic neural networks" *IEEE Trans. Neural Networks*, 3, No.1, 109-118.

Specht D.F., (1991) "A general Regression Neural Network" *IEEE Transactions on Neural Network*, 2, No.6, 568-576.

Specht D.F. (1996) "Fuzzy logic and Neural Network Handbook: Chapter 3- Probabilistic and General Regression Neural Networks" McGraw-Hill Companies, Inc., New York.

Stark T.D. and Olson S.M. (1995) "Liquefaction resistance using CPT and field case histories" Journal of the Geotechnical Engineering Division, ASCE, 121(GT12): 856–869.

Stewart J.P., Chu D.B., Lee S., Tsai J.S., Lin P.S., Chu B.L., Moss R.E.S., Seed R.B., Hsu S.C., Yu M.S., and Wang M.C.H., (2001) "Liquefaction and non-liquefaction from 1999 Chi-Chi, Taiwan, earthquake. *Technical Council on Lifeline Earthquake Engineering*, Monograph No. 25, J.E. Beavers (ed.), pp.1021-1030.

Suzuki Y, Tokimatsu K, Koyamada K, Taya Y, and Kubota Y. Field correlation of soil liquefaction based on CPT data. In Proceedings of the International Symposium on Cone Penetration Testing, Linkoping, Sweden, 1995, Vol. 2, pp. 583–588.

Teh, C. L., Wong, K.S., Goh, A.T.C. and Jaritngam, S. (1997). "Predicting settlement of shallow foundations using neural networks." *Journal of computing in civil engineering*, 11(2), 129-138.

Terzaghi and Peck R. B. (1967) "Soil Mechanics in Engineering Practice" Wiley and Sons, N.Y.

Tokimatsu, K. and Yoshimi, Y. (1983). "Empirical correlation of soil liquefaction based on SPT N-value and fines content." *Soils and Foundations*, 23(4), 56-74.

Ural D.N. and Saka H., (1998) "Liquefaction assessment by neural networks" *Elect. J. Geotech. Eng.*, http://geotech.civen.okstate.edu/ejge/ppr9803/index.html

Youd T.L., Idriss I.M., Andrus R.D., Arango I., Castro G., Christian J.T., Dobry R., Finn W.D., Harder L.F., Hynes M.E., Ishiara K., Koester J.P., liao S.S.C., Marcuson W.F., Martin G.R., Mitchell J.K., Moriwaki Y., Power M.S., Robertson P.K., Seed R.B., and Stokoe K.H., II. (2001) "Liquefaction resistance of soils: Summary report from the 1996 NCEER and 1998 NCEER/NSF Workshops on evaluation of liquefaction resistance of soils" Journal of Geotechnical and Geoenvironmental Engineering, ASCE, 127, No.10, 817-833.

Youd, T. L., and Noble, S. K. (1997). ''Magnitude scaling factors.'' *Proc., NCEER Workshop on Evaluation of Liquefaction Resistance of Soils*, Nat. Ctr. for Earthquake Engrg. Res., State Univ. of New York at Buffalo, 149–165.

Wang, W. (1979). " Some findings in soil liquefaction." Water Conservancy and Hydroelectric Power Scientific Research Institute, Beijing, China.

Wasserman P.D. (1993) "Advanced Methods in Neural Network" Van Nostrand Reinhold, 147-158.